Chapter 4
Master Equations Versus Keldysh Green's Functions for Correlated Quantum Systems Out of Equilibrium

Enrico Arrigoni and Antonius Dorda

Abstract The goal of these lecture notes is to illustrate connections between two widely used, but often separately adopted approaches to deal with quantum systems out of equilibrium, namely quantum master equations and nonequilibrium Green's functions. For the paradigmatic case of the Anderson impurity model out of equilibrium we elaborate on these connections and map its description from one approach to the other. At the end of this chapter, we will show how the "best of the two worlds" can be combined to obtain a highly accurate solution of this model, which resolves the nonequilibrium Kondo physics down to temperatures well below the Kondo scale. As a training course, these lectures devote a large portion to an introduction to the Lindblad quantum master equation based on standard treatments, as well as methods to solve this equation. For nonequilibrium Green's functions, which are discussed in the first part of the course, we only provide a summary of the most important aspects necessary to address the topics of the present chapter. The relevant aspects of these two topics are presented in a self-contained manner so that a background in equilibrium many-body physics is sufficient to follow these notes.

4.1 Introduction

The problem we address in these lectures consists of a small correlated central system in which particles interact with each other, connected to external noninteracting infinite reservoirs (leads), see Fig. 4.1. We focus here to the case of a purely fermionic model, although many ideas can be easily extended to more general problems including, e.g., electron-phonon interactions, photons, etc. We are typically interested in the case of two leads with different chemical potentials and/or temperatures (see, e.g. [1, 2]). Thus, a particle current flows from the lead with larger chemical poten-

E. Arrigoni (✉) · A. Dorda
Graz University of Technology, 8010 Graz, Austria
e-mail: arrigoni@tugraz.at

A. Dorda
e-mail: antonius.dorda@gmx.at

R. Citro and F. Mancini (eds.), *Out-of-Equilibrium Physics of Correlated Electron Systems*, Springer Series in Solid-State Sciences 191,
https://doi.org/10.1007/978-3-319-94956-7_4

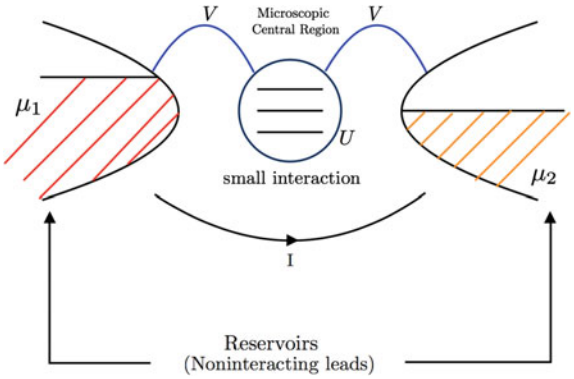

Fig. 4.1 Schematic illustration of the system of interest: A small interacting central system is connected to two leads with different chemical potentials and/or temperatures. The leads are infinite, so that a stationary current flows from one lead to the other in the steady state

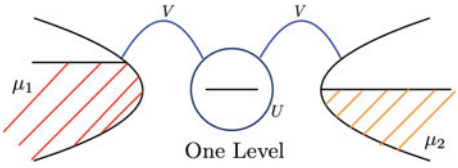

Fig. 4.2 Special case of the system depicted in Fig. 4.1: The single impurity Anderson Model out of equilibrium. The central system consists of a single spin-degenerate level, with on-site Hubbard interaction U. The coupling to the leads is provided by the hopping V

tial through the central system to the other lead, and, since the leads are infinite they provide the dissipation necessary to reach a stationary state. As a paradigmatic example, on which we will focus in the last part of this lecture, we consider the special case of a central system consisting of a single interacting spin-degenerate level with an onsite Hubbard interaction (Fig. 4.2), the single impurity Anderson model (SIAM) [3–7] out of equilibrium. This model is, on the one hand, interesting *per se* as a simple description of transport across quantum dots or small molecules and for understanding the Kondo effect, and on the other hand, constitutes the "bottleneck" problem in the self-consistent cycle within nonequilibrium dynamical mean field theory (DMFT) [8–24], see also previous chapters in this book. Therefore, an accurate solution of impurity models is of great interest and importance.

While we will restrict mainly to the steady state, other related situations can be treated with the approaches presented here and similar ones. For example, one can include a periodic driving within a Floquet approach, or study quantum quenches in which one is interested in the real time dynamics after a sudden change of parameters (see Fig. 4.3).

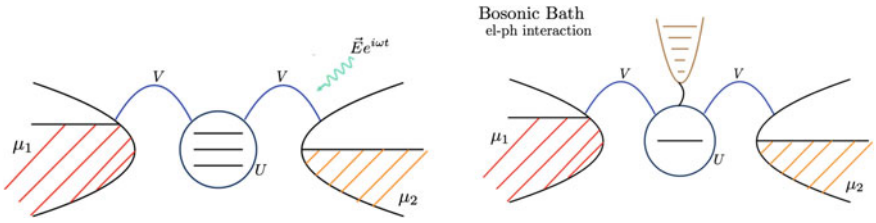

Fig. 4.3 Possible extensions: Time-dependent situations such as quantum quenches [15, 25], i.e. sudden change of parameters, or periodically driven systems [11, 26–29] (left); or coupling to a bosonic bath to account e.g. for electron phonon interaction [30–35] (right)

Limits in which the impurity problem can be solved

Numerous approaches have been developed in the past decades to address impurity problems. For the case of a single reservoir, the steady state corresponds to thermodynamic equilibrium. Dedicated methods such as numerical renormalization group (NRG) were developed in order to resolve the challenging and exponentially small low-energy physics of the model. As a result, the so-called Kondo effect (in equilibrium) is nowadays well understood [7, 36–38]. For the nonequilibrium case a number of numerical approaches have been suggested that are valid in specific limits, but a "full solution" is not yet available. A discussion of all these approaches is beyond the scope of these lectures.[1] Instead, we present in Sect. 4.9 the so-called Auxiliary Master Equation Approach (AMEA) a non-perturbative approach devised and developed in our group in recent years, which is based on a combination of quantum master equation with nonequilibrium Green's functions.

To start with, let consider situations in which models of Figs. 4.1 and 4.2 are exactly solvable. Two trivial cases are (i) the noninteracting case $U = 0$, where one can use nonequilibrium Green's functions, and the decoupled case $V = 0$, for which one can explicitly carry out an exact diagonalization of the many-body Fock space of the small central system. But there is another less trivial limit in which an exact solution is available, the so-called *Markovian Limit*. This is the case when the response of the reservoir is instantaneous, i.e. without memory effects. In this limit, the reservoir's degrees of freedom can be eliminated and the dynamics of the reduced density matrix of the central system is exactly described by the so-called *Lindblad Equation*. Since the central system is small this can again be solved by *exact diagonalization in the space of many-body density matrices*. This will be discussed in detail in Sect. 4.9.1.2.

Outline

The Lindblad equation is the main topic of the first part of the present lectures. More specifically, we will:

[1] For a non-comprehensive list see, e.g., [21, 39–64].

(1) Provide a derivation of the Lindblad Equation, first heuristically in Sect. 4.4.1 and then rigorously in Sect. 4.4.4.
(2) Discuss under which condition a reservoir can be considered as Markovian (Sect. 4.4.4). We will specify this explicitly in terms of the parameters of the microscopic model. As anticipated, we will mainly concentrate on fermionic models.
(3) Present some approaches to solve the many-body Lindblad equation for the non-interacting and the interacting case. In particular, we shall present the so-called superfermion representation [65] (Sect. 4.5), in which the space of density operators for the open system is replaced by a "superspace" of state vectors acting on twice as many single-particle levels (see also [66, 67]). In this formalism, the Lindblad equation acquires a structure like the Schrödinger equation, with which many of us are more familiar.
In the noninteracting case, this linear operator problem can be solved by equations-of-motion techniques, leading to an analytic expression for the steady-state Green's functions, see Sect. 4.9.1.1. In the interacting case we will discuss the solution via exact diagonalization in Sect. 4.9.1.2.

Master Equation Approaches

Unfortunately, it turns out that the Markovian approximation is unrealistic for interesting fermionic models. As we will see, a Markovian reservoir must have both a constant density of states as well as an infinite temperature T and/or chemical potential(s) μ.[2] While these two conditions appear quite restrictive and unphysical, a possible solution is to introduce an intermediate auxiliary buffer zone (mesoreservoir) between the Lindblad couplings and the central system (Sect. 4.8.1, see, e.g. [65, 69, 70] and Fig. 4.4). The buffer zone consists of N_B isolated discrete sites (bath levels), each one coupled to a reservoir with a constant density of states that is either completely filled $\mu = +\infty$ or completely empty $\mu = -\infty$. Therefore, these reservoirs fulfill the Markovian condition and the system can be exactly mapped onto a Lindblad equation. With properly chosen parameters and for large enough N_B, the buffer layer plus Markovian reservoirs exactly describe an *arbitrary non-Markovian* reservoir of noninteracting fermions coupled to the central system [71].[3]

Here comes the connection with nonequilibrium Green's functions[4]: The model as depicted in the lower part of Fig. 4.4 can, on the one hand, be seen as a an open system (the central system plus the buffer layer) whose dynamics is exactly controlled by the Lindblad equation, and on the other hand, consists of a closed system with an infinite number of fermionic levels, that can be (approximately) treated by nonequilibrium Green's functions. For the case of a noninteracting central system, an exact solution is obviously available in both cases. This is shown in Sect. 4.9.1.1, where we will derive analytic expressions for the steady state Green's functions in the noninteracting case.

[2] See also [68].
[3] For related discussions about non-Markovianity and open quantum systems, see e.g. [72–76].
[4] For similar discussions see, e.g. [52, 77].

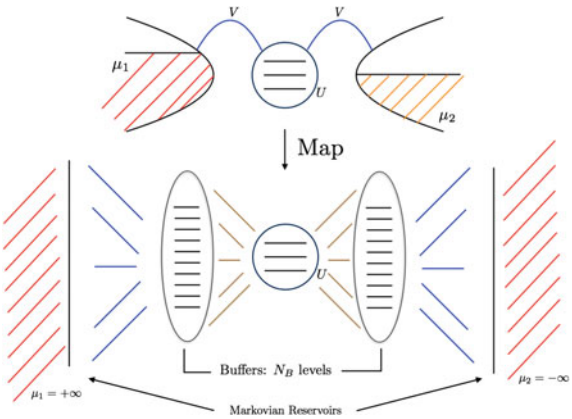

Fig. 4.4 Buffer layer approach: Mapping the original problem onto a system with a finite number of levels, connected in turn to Markovian environments. With appropriate choice of the parameters, the mapping becomes exact for $N_B \to \infty$

The problem we want to address, however, includes an interaction in the central system, which makes an exact solution by Green's function methods impossible. On the other hand, the Lindblad equation for the open system can, in principle, be solved exactly by approaches addressing the full many body space of density matrices, provided N_B is small enough. This will be discussed in Sect. 4.9.1.2. Unfortunately, the buffer layer representation discussed above is limited by the fact that an accurate description of the original system requires quite large values N_B, especially at low temperatures where the Fermi function is sharp. Consequently, the many-body Hilbert space is too large and the treatment of a correlated problem becomes prohibitive.

In the last part of these lectures, Sect. 4.9, we will illustrate how the efficiency of this buffer layer approach can be significantly improved by allowing for more general Lindblad couplings [21, 63, 71, 78], which are determined through an optimization procedure aiming at fitting the so-called bath hybridization function. For the case of the nonequilibrium Anderson impurity model, Fig. 4.2, already modest values of N_B ($N_B \lesssim 8$), which can be treated by Krylov-space schemes [63], are sufficient to resolve the nonequilibrium behavior of the Kondo resonance. Larger values of N_B ($N_B \lesssim 20$) can be addressed by matrix-product states [79–82] which allows to resolve the Kondo peak at temperatures below the Kondo scale with an accuracy that, in equilibrium, becomes comparable with NRG up to intermediate values of the interaction U [78].[5]

4.2 Master Equations

Besides quantum problems, master equations are a central object in classical physics in the context of stochastic processes. Examples are for instance Brownian motion

[5]More specifically, in [78] we resolved temperatures down to $T/T_K = 0.25$ for $T_K = 0.2\Gamma$.

or any other subsystem coupled to a heat bath/environment. In such cases, when the dynamics of a system is non-deterministic it is convenient to describe its state by a probability density. For the case of stochastic processes which fulfill the *Markov* property, i.e. which have a very short memory kernel and only depend on the present state of the system, a master equation is applicable. For a thorough introduction we refer e.g. to [83–85]. Here, we will follow the treatment by Schaller [84].

Let us consider here a discrete set of system states labeled by k and assign each state a probability P_k. The temporal evolution of these probabilities is governed by the rates $T_{kl} \geq 0$ for a transition from state l to state k, and is described by the master equation:

$$\boxed{\frac{dP_k}{dt} = \sum_l \left[T_{kl}P_l - T_{lk}P_k\right]} \tag{4.1}$$

In order for the P_k to be interpreted as probabilities, at each time they have to obey two properties: (i) Conservation of total probability $\sum_k P_k = 1$, and (ii) semipositivity $P_k \geq 0\ \forall k$. Assuming that (i) and (ii) are fulfilled at some initial time, the master equation must guarantee that these properties are preserved.
(i) can be proven as follows:

$$\sum_k \frac{dP_k}{dt} = \sum_{kl} \left(T_{kl}P_l - T_{lk}P_k\right) = \sum_{kl} \left(T_{lk}P_k - T_{lk}P_k\right) = 0\,. \tag{4.2}$$

For (ii) one can argue in the following way. Assume that for a certain k^*, the corresponding P_{k^*} becomes zero at a certain time. Then

$$\left.\frac{dP_{k^*}}{dt}\right|_{P_{k^*}=0} = +\sum_l T_{k^*l}P_l \geq 0\,. \tag{4.3}$$

Therefore, P_{k^*} cannot become negative.

Example Consider the temporal dynamics of a two level system with transition rate T_{10} from state $k = 0$ to state $k = 1$ and rate T_{01} for the inverse process. The master equation (4.1) is in matrix form then given by

$$\frac{d}{dt}\begin{pmatrix} P_0 \\ P_1 \end{pmatrix} = \begin{pmatrix} -T_{10} & +T_{01} \\ +T_{10} & -T_{01} \end{pmatrix}\begin{pmatrix} P_0 \\ P_1 \end{pmatrix}\,. \tag{4.4}$$

The stationary (steady-state) solution P_i^∞ is obtained by setting the left-hand side to zero, yielding

$$\begin{aligned} P_0^\infty &= T_{01}/\left(T_{01} + T_{10}\right)\,, \\ P_1^\infty &= T_{10}/\left(T_{01} + T_{10}\right)\,. \end{aligned} \tag{4.5}$$

The two eigenvalues of the matrix on the right-hand side of (4.4) are 0 and $-\lambda = -T_{01} - T_{10}$. The former corresponds to the stationary solution and λ determines the decay rate in the time evolution. The full time-dependent solution of (4.4) is easily seen to be

$$\begin{aligned} P_0(t) &= P_0(0)e^{-\lambda t} + P_0^{\infty}\left(1 - e^{-\lambda t}\right), \\ P_1(t) &= P_1(0)e^{-\lambda t} + P_1^{\infty}\left(1 - e^{-\lambda t}\right). \end{aligned} \tag{4.6}$$

4.3 Density Matrix

Open quantum systems consist of a microscopic quantum mechanical central system of interest which couples, possibly weakly, with an environment. Due to the entanglement with the environment, the properties of the central system cannot be described by a quantum state alone, but rather require the concept of reduced density matrix. The same concept is also needed if the quantum state of the central system is not known exactly due to a statistical uncertainty. A general mixed system state can be characterized by an ensemble of states $\{|\Phi_i\rangle\}$ which are realized with probability P_i. Here $\sum_i P_i = 1$ and the states are normalized but not necessarily orthogonal. Such a mixed quantum state is conveniently described in terms of the density matrix (or density operator)

$$\rho = \sum_i P_i |\Phi_i\rangle\langle\Phi_i| \,. \tag{4.7}$$

The expectation value of an operator A for the system is then given by

$$\begin{aligned} \langle A\rangle &= \sum_i P_i \langle\Phi_i|A|\Phi_i\rangle \\ &= \sum_{i,n} P_i \langle\Phi_i|n\rangle\langle n|A|\Phi_i\rangle \\ &= \sum_n \langle n|A \underbrace{\sum_i P_i |\Phi_i\rangle\langle\Phi_i|}_{\text{Density matrix}} n\rangle \\ &= \mathrm{Tr} A\rho \,. \end{aligned} \tag{4.8}$$

ρ must fulfill the following properties:

$\langle 1\rangle = 1 \Rightarrow \mathrm{Tr}\rho = 1$	Normalization
$\rho = \rho^{\dagger}$	Hermiticity
$\langle\psi|\rho|\psi\rangle = \sum_i P_i |\langle\psi|\Phi_i\rangle|^2 \geq 0 \quad \forall|\psi\rangle$	(Semi) positivity: $\rho \geq 0$

If the system is characterized by a single quantum mechanical state with probability 1, the density matrix describes a so-called pure state for which

$$\rho = |\Phi_i\rangle\langle\Phi_i| \Rightarrow \rho^2 = \rho\,. \tag{4.9}$$

On the other hand, for a general non-pure (mixed) state $\rho = \sum_n P_n|\psi_n\rangle\langle\psi_n|$ expanded in its eigenbasis[6] one finds

$$\begin{aligned} \mathrm{Tr}\rho^2 &= \sum_{m,n,k} \langle\psi_m|\psi_n\rangle\langle\psi_n|\psi_k\rangle\langle\psi_k|\psi_m\rangle P_n P_k \\ &= \sum_n P_n^2 \leq 1. \end{aligned} \tag{4.10}$$

Therefore, a system is in a pure state if and only if

$$\mathrm{Tr}\rho^2 = 1 \tag{4.11}$$

so that $\mathrm{Tr}\rho^2$ is a measure for the degree of purity of the state [86].

4.3.1 Time Dependence

The time evolution of the density matrix ρ for a *closed* quantum system is determined by the Liouville von Neumann Equation[7]:

$$\begin{aligned} \dot{\rho} &= \sum_i P_i \left(|\dot{\Phi}_i\rangle\langle\Phi_i| + |\Phi_i\rangle\langle\dot{\Phi}_i|\right) \\ &= -i[H, \rho]\,, \end{aligned} \tag{4.12}$$

which can be easily obtained by applying the Schrödinger equation for $|\dot{\Phi}_i\rangle$, and using $\dot{P}_i = 0$. Notice that (4.12) is similar to the Heisenberg time evolution for an operator, $\dot{A} = +i[H, A]$, however, the sign is opposite.

It is easy to verify that (4.12) preserves normalization, Hermiticity and semipositivity of the density matrix:

$$\mathrm{Tr}\rho = 1 \qquad \rho = \rho^\dagger \qquad \rho \geq 0\,, \tag{4.13}$$

An important example for a nonunitary evolution is a measure operation. Let us consider the spectral representation of a generic operator A,[8]

[6] In contrast to the $|\Phi_i\rangle$ in (4.7) the $|\psi_n\rangle$ are orthogonal to each other.

[7] From now on we will adopt units in which $\hbar = 1$.

[8] In these lectures, we will not explicitly mark operators with a hat "ˆ" except when there is a risk of confusion.

$$A = \sum_n a_n \hat{P}_n,$$
$$\hat{P}_n \equiv |a_n\rangle\langle a_n|, \tag{4.14}$$

with $\hat{P}_n$ the projection operators onto the eigenstates $|a_n\rangle$, of A, i.e. $A|a_n\rangle = a_n|a_n\rangle$. Quantum mechanics tells us that if one measures A on a pure state $|\Phi_i\rangle$, the value a_n is obtained with probability $P_n = |\hat{P}_n|\Phi_i\rangle|^2$, and the state collapses to

$$|\Phi_i\rangle \to \frac{\hat{P}_n|\Phi_i\rangle}{\sqrt{P_n}}\,. \tag{4.15}$$

Therefore, when starting from $\rho = |\Phi_i\rangle\langle\Phi_i|$ and performing a measure without looking at the result one gets an ensemble of states with the probabilities P_n, i.e.

$$\begin{aligned}\rho \xrightarrow{\text{Measure}} & \sum_n P_n \left(\frac{\hat{P}_n|\Phi_i\rangle}{\sqrt{P_n}}\right)\left(\frac{\langle\Phi_i|\hat{P}_n}{\sqrt{P_n}}\right) \\ = & \sum_n \hat{P}_n|\Phi_i\rangle\langle\Phi_i|\hat{P}_n = \sum_n \hat{P}_n\rho\hat{P}_n\,.\end{aligned} \tag{4.16}$$

Clearly, the last line of (4.16), the *von Neumann measure*, holds also in the case in which one starts from a mixed state ρ. Also in the case of a von Neumann measure, the properties (4.13) are preserved.

Unitary evolution and von Neumann measure are two examples of *quantum operations*, i.e. linear time evolutions for the density matrix.

Example The density matrix of a spin 1/2 system, or any other two-state quantum system, can be represented in terms of the so-called Bloch sphere. The density matrix for such a system can be expressed in terms of the identity I and the Pauli matrices $\boldsymbol{\sigma}$

$$\rho = \frac{1}{2}(I + \boldsymbol{\alpha}\cdot\boldsymbol{\sigma}), \tag{4.17}$$

with $\boldsymbol{\alpha}$ an appropriate vector with real coefficients. From

$$\begin{aligned}\mathrm{Tr}\rho^2 &= \frac{1}{4}\,\mathrm{Tr}\left(I + 2\boldsymbol{\alpha}\cdot\boldsymbol{\sigma} + (\boldsymbol{\alpha}\cdot\boldsymbol{\sigma})^2\right) \\ &= \frac{1}{4}(2 + 2|\alpha|^2)\,,\end{aligned} \tag{4.18}$$

using $\mathrm{Tr}\sigma_i\sigma_j = 2\delta_{ij}$, one finds that $|\boldsymbol{\alpha}| = 1$ describes a pure state, while a mixed state has $|\boldsymbol{\alpha}| < 1$.

4.3.2 Reduced Density Matrix

Open quantum systems consist of a microscopic system embedded within a reservoir, see also Fig. 4.5. In general, one is not interested in the properties of the reservoir itself, however, the latter affect the dynamics of the system. Ideally, one would like to eliminate the degrees of freedom of the reservoir and obtain an effective description for the system alone. Due to the entanglement with the reservoir, the system's quantum mechanical state must be formulated in terms of the so-called reduced density matrix, which, quite generally, describes a mixed state.

The combined Hilbert space of the so-called "universe" (= system + reservoir) is given by the *tensor product space* of the system and the reservoir Hilbert spaces $\mathcal{H}_S$ and $\mathcal{H}_R$:

$$\mathcal{H}_U = \mathcal{H}_S \otimes \mathcal{H}_R. \tag{4.19}$$

A basis of $\mathcal{H}_U$ is $\{|S_i\rangle \otimes |R_\alpha\rangle\}$, where $\{|S_i\rangle\}$ is a basis of $\mathcal{H}_S$ and $\{|R_\alpha\rangle\}$ a basis of $\mathcal{H}_R$. For simplicity, we will use alternative equivalent notations

$$|S_i\rangle \otimes |R_\alpha\rangle \leftrightarrow |S_i\rangle|R_\alpha\rangle \leftrightarrow |S_i, R_\alpha\rangle\,, \tag{4.20}$$

and for the bra counterparts

$$\langle S_i| \otimes \langle R_\alpha| \leftrightarrow \langle S_i|\langle R_\alpha| \leftrightarrow \langle S_i|\langle R_\alpha|\,.$$

Let us recall the following important properties of the tensor product:

- Distributivity:

$$\begin{aligned}(|a\rangle + |b\rangle) \otimes |c\rangle &= |a\rangle \otimes |c\rangle + |b\rangle \otimes |c\rangle \\ &= |a, c\rangle + |b, c\rangle\end{aligned} \tag{4.21}$$

- Operators act only on states in their corresponding subspace:

$$(A \otimes B)|x\rangle \otimes |y\rangle = (A|x\rangle) \otimes (B|y\rangle) \tag{4.22}$$

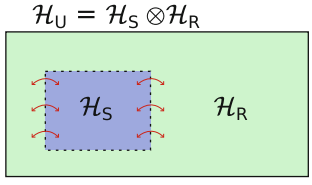

Fig. 4.5 Open system embedded into a reservoir. The Hilbert space for the full "universe" is given by $\mathcal{H}_U = \mathcal{H}_S \otimes \mathcal{H}_R$, for which a pure state description in terms of a wave function is possible. Due to particle/energy exchange between the system and the reservoir this is not true for $\mathcal{H}_S$ and $\mathcal{H}_R$ separately, which requires a description in terms of density matrices

- Scalar Product:

$$(\langle a| \otimes \langle b|) \otimes (|x\rangle \otimes |y\rangle) = \langle a|x\rangle\langle b|y\rangle \tag{4.23}$$

As noted above, the set of product states (4.20) provides a complete basis for $\mathcal{H}_U$. However, a generic state in $\mathcal{H}_U$ will not factorize in simple product states in terms of the system and the reservoir separately. One then speaks of *entangled states*. As an example, let us consider two basis states for the system and the reservoir each, $|S_i\rangle$ and $|R_\alpha\rangle$, $i, \alpha = 1, 2$ and the following two states:

$$\begin{aligned} |\psi_P\rangle &= |S_1\rangle|R_1\rangle + |S_2\rangle|R_1\rangle \\ &= (|S_1\rangle + |S_2\rangle)|R_1\rangle, \end{aligned} \tag{4.24}$$

and

$$\begin{aligned} |\psi_E\rangle &= |S_1\rangle|R_1\rangle + |S_2\rangle|R_2\rangle \\ &\neq |a\rangle|b\rangle. \end{aligned} \tag{4.25}$$

While $|\psi_p\rangle$ is a product state, the latter is not.

From the properties (4.22) and (4.23) one can compute the trace of a tensor product operator $\hat{O} = \hat{A} \otimes \hat{B}$ as

$$\begin{aligned} \mathrm{Tr}\hat{O} &= \sum_{i,\alpha} \langle S_i, R_\alpha|\hat{O}|S_i, R_\alpha\rangle \\ &= \sum_{i,\alpha} \langle S_i|\hat{A}|S_i\rangle\langle R_\alpha|\hat{B}|R_\alpha\rangle \\ &= \underbrace{\mathrm{Tr}\hat{A}}_{\mathrm{Tr}_S}\underbrace{\mathrm{Tr}\hat{B}}_{\mathrm{Tr}_R}. \end{aligned} \tag{4.26}$$

In the last line we introduced the partial traces over either system or reservoir states, defined as:

$$\begin{aligned} \mathrm{Tr}_S\,\hat{O} &= \sum_i \langle S_i|\hat{O}|S_i\rangle, \\ \mathrm{Tr}_R\,\hat{O} &= \sum_\alpha \langle R_\alpha|\hat{O}|R_\alpha\rangle. \end{aligned} \tag{4.27}$$

Let us consider for instance the operator $\hat{O} = |S\rangle\langle S'| \otimes |R\rangle\langle R'|$ and evaluate

$$\begin{aligned} \mathrm{Tr}_R\hat{O} &= |S\rangle\langle S'| \sum_\alpha \langle R_\alpha|R\rangle\langle R'|R_\alpha\rangle \\ &= |S\rangle\langle S'|\,\mathrm{Tr}_R|R\rangle\langle R'|. \end{aligned} \tag{4.28}$$

From this one sees that the partial trace Tr_R produces an operator acting in $\mathcal{H}_S$ alone. An explicit expression for the partial trace of an arbitrary operator $\hat{O}$ expanded in the product basis (4.20)

$$\hat{O} = \sum_{i,\alpha,j,\beta} O_{i,\alpha,j,\beta} |S_i\rangle|R_\alpha\rangle\langle S_j|\langle R_\beta|$$

can be readily obtained as

$$\mathrm{Tr}_R \hat{O} = \sum_{i,j} \left(\sum_{\alpha} O_{i,\alpha,j,\alpha} \right) |S_i\rangle\langle S_j|. \tag{4.29}$$

If we are interested in observables of the system only we can restrict to the system's *reduced density matrix*

$$\rho_S = \mathrm{Tr}_R \rho, \tag{4.30}$$

which is obtained as the partial trace of the density matrix ρ of the universe over the reservoir degrees of freedom. Indeed, the expectation value of an arbitrary operator $A \otimes I$ acting on the system only can be expressed as

$$\begin{aligned} \langle A \otimes I \rangle &= \mathrm{Tr}\left\{ (A \otimes I)\rho \right\} \\ &= \sum_{i,\alpha} \left(\langle S_i| A \otimes \langle R_\alpha| \right) \rho \left(|S_i\rangle \otimes |R_\alpha\rangle \right) \\ &= \sum_{i} \langle S_i| A \sum_{\alpha} \langle R_\alpha|\rho|R_\alpha\rangle |S_i\rangle \\ &= \sum_{i} \langle S_i| A (\mathrm{Tr}_R \rho) |S_i\rangle \\ &= \mathrm{Tr}_S A \rho_S, \end{aligned} \tag{4.31}$$

which is valid for any system operator A. The reduced density matrix, thus, contains all the necessary information to compute system properties. Quite generally, for the universe one can assume that the density matrix is represented by a pure state $\rho = |\psi\rangle\langle\psi|$. On the contrary, the reduced system density matrix $\rho_S = \mathrm{Tr}_R |\psi\rangle\langle\psi|$ only describes a pure state if the universe wave function is a product state: $|\psi\rangle = |R\rangle|S\rangle$. In the general case, when $|\psi\rangle$ is entangled, ρ_S describes a mixed state with $\mathrm{Tr}\rho_S^2 < 1$.

On the other hand, for every given system density matrix ρ_S one can always construct a "sufficiently large" universe $\mathcal{H}_U = \mathcal{H}_S \otimes \mathcal{H}_R$ such that

$$\rho_S = \mathrm{Tr}_R |\psi\rangle\langle\psi|, \tag{4.32}$$

and with $|\psi\rangle$ a pure state. This procedure is termed *purification*. For example, suppose we have $\rho_S = \sum_{n=1}^{N} P_n |\Phi_n\rangle\langle\Phi_n|$. In this case one needs a reservoir with an

N-dimensional orthonormal basis set $\{|R_n\rangle\}$. A universe wave function $|\psi\rangle$ satisfying (4.32) is then, for instance, given by

$$|\psi\rangle = \sum_n \sqrt{P_n}|\Phi_n\rangle \otimes |R_n\rangle \ .$$

Proof

$$\begin{aligned} \mathrm{Tr}_R|\psi\rangle\langle\psi| &= \sum_{n,m} \sqrt{P_n}\sqrt{P_m}|\Phi_n\rangle\langle\Phi_m| \underbrace{\mathrm{Tr}_R|R_n\rangle\langle R_m|}_{\delta_{n,m}} \ . \\ &= \rho_S \end{aligned}$$

The above examples show that there can be two situations in which the quantum mechanical state $|\psi\rangle$ is not sufficient to describe a microscopic system and one needs a density matrix:

1. The exact state is not known, only its statistical distribution.
2. The system is entangled with a reservoir.

In the rest of these lectures we will be interested in the second case.

4.4 Lindblad Equation

As discussed in the previous section, the reduced density matrix contains all possible information about a microscopic system even if it is in contact (entangled) with a large reservoir. This is obviously a big advantage since one has to deal with a much smaller Hilbert space, without caring about the much larger reservoir. However, computing the time evolution of the reduced density matrix is again a prohibitive task. Whenever there is a coupling between system and environment, ρ_S does not evolve according to the Liouville equation (4.12). To find its time evolution one should first evolve the density matrix of the universe ρ, which follows the Liouville equation, and then carry out the partial trace (4.29). The intermediate step, thus, involves again addressing the full universe Hilbert space. It would be useful if, under some conditions, one could work in the restricted subspace of the system reduced density matrices including the action of the reservoir in some effective way. In this section, we are going to show that within the so-called *Markovian condition* one can indeed formulate the time evolution of the reservoir within a closed time evolution equation for ρ_S, the *Lindblad equation*. In Sect. 4.4.4 we will present a microscopic derivation of the Lindblad equation in the so-called strong-coupling limit, and discuss under which conditions, in terms of the parameters of the microscopic model, this equation provides an exact description of the effects of the environment. A microscopic derivation, as well as a derivation obtained by the conventional Markovian assumption based on so-called Kraus operators can be found in several textbooks, see, e.g. [83–85, 87, 88]. Here we will roughly follow the treatments of [84, 88].

But before becoming rigorous, we first present a heuristic derivation based on the master equation discussed in Sect. 4.2.

4.4.1 Heuristic Derivation

A situation described in Sect. 4.3 in which one has a set of quantum-mechanical states $|k\rangle$ occupied with probabilities P_k (also called populations) is described by a density matrix with diagonal elements $\rho_{k,k} = P_k$. As a consequence, the Master equation (4.1) can be rewritten as

$$\left.\frac{d\,\rho_{kk}}{dt}\right|_{Master} = \sum_l (T_{kl}\rho_{ll} - T_{lk}\rho_{kk}), \tag{4.33}$$

The transitions between different states in (4.33) can be expressed in terms of *jump operators*

$$\hat{J}_{kl} = |k\rangle\langle l|. \tag{4.34}$$

This allows to express (4.33) in operator form

$$\left.\frac{d\,\hat{\rho}}{dt}\right|_{Master} = \sum_{l,k} (T_{kl}\hat{J}_{kl}\hat{\rho}\hat{J}_{kl}^\dagger - T_{lk}\hat{J}_{kk}\hat{\rho}). \tag{4.35}$$

In order to have an expression which is quadratic in $\hat{J}$, we rewrite $\hat{J}_{kk} = \hat{J}_{kn}\hat{J}_{nk} = \hat{J}_{nk}^\dagger\hat{J}_{nk}$ with arbitrary n. Accordingly, the term $\hat{J}_{kk}\hat{\rho}$ can be written in several forms, for instance $\hat{J}_{lk}^\dagger\hat{J}_{lk}\hat{\rho}$ or $\hat{\rho}\hat{J}_{lk}^\dagger\hat{J}_{lk}$. While these give the same result for the diagonal terms (4.33), different results are obtained for the nondiagonal terms. We here choose[9] the symmetrized form

$$\hat{J}_{kk}\hat{\rho} \to \frac{1}{2}\left\{\hat{J}_{lk}^\dagger\hat{J}_{lk}, \hat{\rho}\right\}, \tag{4.36}$$

leading to

$$\left.\frac{d\,\hat{\rho}}{dt}\right|_{Master} = \sum_{l,k} T_{kl}\left(\hat{J}_{kl}\hat{\rho}\hat{J}_{kl}^\dagger - \frac{1}{2}\left\{\hat{J}_{kl}^\dagger\hat{J}_{kl}, \hat{\rho}\right\}\right). \tag{4.37}$$

We now replace the jump operators by arbitrary operators

$$J_{kl} \to \bar{S}_n$$

[9] Remember, this is just a non-rigorous derivation.

with corresponding coefficients

$$T_{kl} \to \bar{\gamma}_n$$

and omit the "hats" for the sake of readability. In addition to the master equation (4.33), which describes changes in population of the states, one has to include the Liouville von Neumann contribution (4.12) originating from the internal Hamiltonian dynamics, which leads to

$$\frac{d\rho}{dt} = -i\,[H,\rho] + \sum_n \bar{\gamma}_n \left(\bar{S}_n \rho \bar{S}_n^\dagger - \frac{1}{2}\left\{ \bar{S}_n^\dagger \bar{S}_n, \rho \right\} \right). \tag{4.38}$$

This is the *Lindblad equation* in diagonal form.

The positivity of probabilities is ensured by using nonnegative coefficients $\bar{\gamma}_n$. This allows them to be absorbed into the definition of the $\bar{S}_n$ operators

$$\Gamma_n = \sqrt{\bar{\gamma}_n}\bar{S}_n, \tag{4.39}$$

so that (4.38) can be written as

$$\frac{d\rho}{dt} = -i\,[H,\rho] + \sum_n \left(\Gamma_n \rho \Gamma_n^\dagger - \frac{1}{2}\left\{ \Gamma_n^\dagger \Gamma_n, \rho \right\} \right). \tag{4.40}$$

Besides the diagonal form (4.40), also a non-diagonal one is often adopted:

$$\frac{d\rho}{dt} = -i\,[H,\rho] + \sum_{\alpha\beta} \gamma_{\alpha\beta} \left(S_\beta \rho S_\alpha^\dagger - \frac{1}{2}\left\{ S_\alpha^\dagger S_\beta, \rho \right\} \right), \tag{4.41}$$

where the coefficient matrix $\gamma_{\alpha\beta}$ is Hermitian and semi-positive definite. As can be easily checked, the two forms are linked by the eigen decomposition $\gamma_{\alpha\beta} = \sum_n U_{\alpha,n}^\dagger \bar{\gamma}_n U_{n,\beta}$ and the linear combination $\bar{S}_n = \sum_\alpha U_{n,\alpha} S_\alpha$.

The Lindblad equations (4.38), (4.40) and (4.41) can be formally written in the following form

$$\begin{aligned} \frac{d\hat{\rho}}{dt} &= \hat{\hat{\mathcal{L}}}\hat{\rho} \\ &= \hat{\hat{\mathcal{L}}}_H \hat{\rho} + \hat{\hat{\mathcal{L}}}_D \hat{\rho}. \end{aligned} \tag{4.42}$$

Here, we have introduced a notation with two hats to indicate a superoperator ($\hat{\hat{\mathcal{L}}}$), i.e. a linear transformation in the space of operators (here density matrices). As for operators, we will use the "hat" notation only when necessary in order to avoid confusion. In (4.42) $\hat{\hat{\mathcal{L}}}_H$ describes the Liouville von Neumann contribution and thus

unitary time evolution, while $\hat{\hat{\mathcal{L}}}_D$ is the so-called dissipator. It is straightforward to prove (see, e.g. [83, 84]) that the Lindblad equation preserves the properties of the density matrix, namely

$$\mathrm{Tr}\rho = 1 \qquad \rho = \rho^\dagger \qquad \rho \geq 0\,. \tag{4.43}$$

4.4.2 *Solution of the Lindblad Equation by Exact Diagonalization*

The formal solution of the linear equation (4.42), for the case of a time-independent $\hat{\hat{\mathcal{L}}}$, is obtained in the usual way:

$$\hat{\rho}(t) = e^{\hat{\hat{\mathcal{L}}}t}\hat{\rho}(0). \tag{4.44}$$

Or, in terms of the eigenoperators $\hat{\rho}^{(\alpha)}$ and corresponding eigenvalues $\mathcal{L}_\alpha$ of $\hat{\hat{\mathcal{L}}}$, satisfying

$$\hat{\hat{\mathcal{L}}}\hat{\rho}^{(\alpha)} = \mathcal{L}_\alpha\hat{\rho}^{(\alpha)}, \tag{4.45}$$

one has

$$\hat{\rho}(t) = \sum_\alpha c_\alpha \hat{\rho}^{(\alpha)} e^{\mathcal{L}_\alpha t}, \tag{4.46}$$

where the c_α are fixed by the initial $t = 0$ condition. Since $\hat{\hat{\mathcal{L}}}$ is *non-Hermitian* its eigenvalues are complex, so we write them as

$$\mathcal{L}_\alpha = R_\alpha + iI_\alpha. \tag{4.47}$$

From (4.46) we readily see that we must have $R_\alpha \leq 0$ since otherwise there would be unphysical exponential divergences at large times. The coefficients $-R_\alpha$ are the decay rates of the exponentially damped modes described by the corresponding $\hat{\rho}^{(\alpha)}$. In order for the trace to be preserved, at least one eigenvalue, say the one with $\alpha = 0$, is expected to be zero,[10] $\mathcal{L}_{\alpha=0} = 0$. Then $\hat{\rho}^{(\alpha=0)}$ corresponds to the stationary or steady state which survives in the long-time limit.

Alternatively, instead of addressing the full "doubled" many-body space of the density matrix, one can use quantum trajectory methods [82, 89–92], whereby the density matrix is replaced by an ensemble of quantum states and the dissipative terms of the Lindblad equation produces so-called quantum jumps.

[10] Or one or more must have $R_\alpha = 0$.

4.4.3 Fermionic Model Described by the Lindblad Equation

We are here interested in the situation of a fermionic central system connected to a reservoir of non-interacting fermions. We will later show that under some conditions, the action of the reservoir can be described by a correction to the system's Hamiltonian (Lamb shift) plus a dissipator [cf. (4.41)]

$$\begin{aligned}\mathcal{L}_D\rho = &\sum_{i,j} 2\Gamma_{1ij}\left(a_j\rho a_i^\dagger - \frac{1}{2}\left\{a_i^\dagger a_j, \rho\right\}\right)\\ &+\sum_{i,j} 2\Gamma_{2ij}\left(a_i^\dagger\rho a_j - \frac{1}{2}\left\{a_j a_i^\dagger, \rho\right\}\right).\end{aligned} \tag{4.48}$$

Here, ρ is the reduced density matrix of the central system. This becomes an exact description of the reservoir in particular limits, as discussed below. The terms in (4.48) proportional to Γ_{1ij} with jump operators a_j describe particles jumping from the central system into the reservoir. The ones with Γ_{2ij} describe the opposite process, namely particles jumping from the reservoir into the central system.

Example As an example, consider a single-level model [(4.48) with no indices i and j], for which the Hamiltonian reads

$$H = \varepsilon a^\dagger a. \tag{4.49}$$

By explicitly solving for the steady-state of the Lindblad equation it is straightforward to show that the steady state occupation reads

$$\langle a^\dagger a\rangle = \frac{\Gamma_2}{\Gamma_1+\Gamma_2} \tag{4.50}$$

4.4.4 Microscopic Derivation of the Lindblad Equation

In this section we will provide an explicit derivation of (4.41) starting from a microscopic model describing a central system coupled to a reservoir. In (4.41), ρ is the reduced density matrix of the central system after tracing out the reservoir. This topic has been treated in a number of textbooks. Here, we roughly follow [84, 88].

We start from a "universe" consisting of a central system +reservoir and described by the following Hamiltonian

$$H = H_S\otimes I + I\otimes H_R + V = H_0 + V. \tag{4.51}$$

Here, H_S (H_R) is the Hamiltonian for the isolated central system (reservoir), and V is the coupling between the two. The latter can always be expressed in terms of a

sum of tensor products of system (S_α) and reservoir (R_α) operators:

$$V = v \sum_\alpha S_\alpha \otimes R_\alpha . \tag{4.52}$$

The parameter v is introduced for convenience as a measure for the strength of the coupling V, and will be used later in order to discuss the range of validity of the Lindblad equation. v is chosen in such a way that the operators S_α and R_α are of order 1. The full density matrix ρ for the (closed) universe obeys the Liouville-von Neumann equation

$$\dot{\rho} = -i \left[H_0 + V, \rho \right] . \tag{4.53}$$

The goal is to integrate out the reservoir degrees of freedom in order to arrive at an effective time evolution equation for the reduced density matrix

$$\rho_S(t) = \mathrm{Tr}_R \rho(t), \tag{4.54}$$

which only depends on system operators and $\rho_S(t)$ itself. As we will show on the next pages, under certain conditions one gets an equation of Lindblad form

$$\frac{d\,\hat{\rho}_S(t)}{dt} = \hat{\hat{\mathcal{L}}} \hat{\rho}_S(t). \tag{4.55}$$

A central aspect is that this equation is time local, which is a consequence of the so-called *Markovian* assumption for the reservoirs' dynamics, see below, so that memory effects are neglected.

A trivial limit is the decoupled case $V = 0$. Here, the time evolution for $\rho_S(t)$ is unitary and the Lindblad equation is given by

$$\frac{d}{dt} \hat{\rho}_S = -i \left[\hat{H}_S, \hat{\rho}_S \right] . \tag{4.56}$$

Introducing the density matrix in the interaction picture

$$\bar{\rho}(t) \equiv e^{iH_0 t} \rho(t) e^{-iH_0 t}, \tag{4.57}$$

Equation (4.53) can be rewritten as

$$\dot{\bar{\rho}} = -i \left[\bar{V}(t), \bar{\rho} \right], \tag{4.58}$$

where

$$\begin{aligned} \bar{V}(t) &= e^{iH_0 t} V e^{-iH_0 t} \\ &= v \sum_\alpha S_\alpha(t) \otimes R_\alpha(t), \end{aligned} \tag{4.59}$$

is the system-reservoir coupling in the interaction picture, and the time evolution of $S_\alpha(t)$[11] is determined by its corresponding unperturbed Hamiltonian, i.e. $S_\alpha(t) = e^{iH_S t} S_\alpha e^{-iH_S t}$, and similarly for R_α.

4.4.4.1 Born Markov Approximation

According to (4.58), the time evolution for a small step Δt is given by

$$\bar{\rho}(t+\Delta t) = -i \int_t^{t+\Delta t} \left[\bar{V}(t'), \bar{\rho}(t')\right] dt' + \bar{\rho}(t). \tag{4.60}$$

This equation can be iterated by inserting for $\bar{\rho}(t')$ again (4.60), leading to

$$\Delta\bar{\rho}(t) = -i \int_t^{t+\Delta t} \left[\bar{V}(t'), \bar{\rho}(t)\right] dt' - \int_t^{t+\Delta t} dt' \int_t^{t'} dt'' \left[\bar{V}(t'), \left[\bar{V}(t''), \bar{\rho}(t'')\right]\right], \tag{4.61}$$

where $\Delta\bar{\rho}(t) \equiv \bar{\rho}(t+\Delta t) - \bar{\rho}(t)$. We now split $\bar{\rho}$ in the following way:

$$\bar{\rho}(t) = \bar{\rho}_S(t) \otimes \bar{\rho}_{R0}(t) + \delta\bar{\rho}_{corr}(t), \tag{4.62}$$

where, $\bar{\rho}_S(t) \equiv \mathrm{Tr}_R \bar{\rho}(t)$ is the system's reduced density matrix, $\bar{\rho}_{R0}(t)$ the unperturbed ($V = 0$) reservoir density matrix, and $\delta\bar{\rho}_{corr}$ the rest, which accounts for correlations between system and reservoir. $\bar{\rho}_{R0}(t)$ is chosen to commute with H_R, so that it is time independent $\bar{\rho}_{R0}(t) \to \rho_R$. This is not a major restriction and, for example, this is the case for the equilibrium distribution $\rho_R \propto e^{-\beta H_R}$.

The main approximation now will be to neglect $\delta\bar{\rho}_{corr}$. In Sect. 4.4.4.3 we will discuss under which conditions and in what sense this is justified. With this approximation, (4.61) becomes

$$\begin{aligned}\Delta\bar{\rho}_S(t) = &-i \int_t^{t+\Delta t} dt' \mathrm{Tr}_R \left[\bar{V}(t'), \bar{\rho}_S(t') \otimes \rho_R\right] \\ &- \int_t^{t+\Delta t} dt' \int_t^{t'} dt'' \mathrm{Tr}_R \left[\bar{V}(t'), \left[\bar{V}(t''), \bar{\rho}_S(t'') \otimes \rho_R\right]\right].\end{aligned} \tag{4.63}$$

The first term on the r.h.s. of (4.63) can generally be taken to be zero. Specifically, this part contains terms of the form

$$\mathrm{Tr}_R R_\alpha(t') \rho_R = \mathrm{Tr}_R R_\alpha \rho_R = r_\alpha, \tag{4.64}$$

[11] We omit the bar used to indicate the interaction picture here, since this is already clear from the time dependence.

and the numbers r_α can be chosen without restriction to be zero. Indeed, for nonzero r_α one may introduce new reservoir operators

$$R'_\alpha = R_\alpha - r_\alpha \mathbb{1}, \tag{4.65}$$

which yield $\mathrm{Tr}_R R'_\alpha \rho_R = 0$. The coupling Hamiltonian (4.52) becomes

$$V = v \sum_\alpha \left(R'_\alpha \otimes S_\alpha + r_\alpha S_\alpha \right), \tag{4.66}$$

and the term $v \sum_\alpha r_\alpha S_\alpha$ can be reabsorbed into H_S.

To get a useful expression out of the remaining term in (4.63) (second line), we need to introduce the *Markov* approximation. In order to understand it, let us denote by T_S the time scale over which the system, i.e. $\bar{\rho}_S$, changes due to the interaction with the environment. In terms of $\bar{\rho}_S$ this is clearly given by

$$T_S \sim \left(\frac{|\Delta \bar{\rho}_S|}{\Delta t} \frac{1}{|\bar{\rho}_S|} \right)^{-1}, \tag{4.67}$$

where $|\cdots|$ is some suitable measure. We now take Δt, which up to now can be chosen arbitrarily, to be

$$\Delta t \ll T_S. \tag{4.68}$$

In this way, since the variation of $\bar{\rho}_S(t'')$ for $t \le t'' \le t + \Delta t$ is negligible, one can replace in (4.63) $\bar{\rho}_S(t'') \to \bar{\rho}_S(t)$. With this one obtains from (4.63) the coarse-grained derivative

$$\frac{\Delta \bar{\rho}_S(t)}{\Delta t} = -\frac{1}{\Delta t} \int_t^{t+\Delta t} dt' \int_t^{t'} dt'' \, \mathrm{Tr}_R \Big[\bar{V}(t'), \Big[\bar{V}(t''), \bar{\rho}_S(t) \otimes \rho_R \Big] \Big]. \tag{4.69}$$

This equation looks *Markovian*, as $\bar{\rho}_S(t)$ is time local and there is no memory on the past. However, this is valid only in a very small interval Δt, and we will see below that Δt cannot be taken arbitrarily small.

4.4.4.2 Reservoir Correlation Functions

Equation (4.69) contains terms of the form

$$\mathrm{Tr}_R R_\alpha(t') R_\beta(t'') \rho_R \equiv C_{\alpha\beta}(t' - t''), \tag{4.70}$$

and permutations thereof. Here, we have again exploited time translational invariance of the reservoir. Provided the reservoir is infinite, its correlation functions $C_{\alpha\beta}(\tau)$

decay with a characteristic time scale τ_R. As we will see, in order to be able to neglect $\delta\bar{\rho}_{corr}$, one must have

$$\tau_R \ll \Delta t. \tag{4.71}$$

This has to be supplemented with the previous requirement $\Delta t \ll T_S$. More specifically, we will see (cf. [88]) that if (4.71) is fulfilled, the contribution from $\delta\bar{\rho}_{corr}$ are canceled from coarse graining on the scale Δt.

Introducing the time difference $\tau = t' - t'' \in (0, \Delta t)$, the integrals in (4.69) can be rewritten as

$$\int_0^{\Delta t} d\tau \int_{t+\tau}^{t+\Delta t} dt' \ldots. \tag{4.72}$$

The integrand contains terms $C_{\alpha\beta}(\tau)$, which decay in a time $\tau_R \ll \Delta t$. Therefore, it is safe to change the boundaries of the integrals to

$$\int_0^{\infty} d\tau \int_{t}^{t+\Delta t} dt' \ldots \tag{4.73}$$

With the explicit form of the coupling Hamiltonian (4.52), (4.69) becomes

$$\begin{aligned}\frac{\Delta\bar{\rho}_S(t)}{\Delta t} = -\int_0^{\infty} d\tau \frac{1}{\Delta t}\int_t^{t+\Delta t} dt' v^2 \sum_{\alpha\beta}\Big\{ & S_\alpha(t')S_\beta(t'-\tau)\bar{\rho}_S(t)C_{\alpha\beta}(\tau) \\ & -S_\alpha(t')\bar{\rho}_S(t)S_\beta(t'-\tau)C_{\beta\alpha}(-\tau) \\ & -S_\beta(t'-\tau)\bar{\rho}_S(t)S_\alpha(t')C_{\alpha\beta}(\tau) \\ & +\bar{\rho}_S(t)S_\beta(t'-\tau)S_\alpha(t')C_{\beta\alpha}(-\tau)\Big\}.\end{aligned} \tag{4.74}$$

From here we shall omit to explicitly indicate the time argument for $\bar{\rho}_S(t)$. Equations (4.74) in turn can be rewritten in terms of commutators as

$$\begin{aligned}\frac{\Delta\bar{\rho}_S}{\Delta t} = -\int_0^{\infty} d\tau \frac{1}{\Delta t}\int_t^{t+\Delta t} dt' v^2 \sum_{\alpha\beta}\Big\{ & C_{\alpha\beta}(\tau)\Big[S_\alpha(t'), S_\beta(t'-\tau)\bar{\rho}_S\Big] \\ & +C_{\beta\alpha}(-\tau)\Big[\bar{\rho}_S S_\beta(t'-\tau), S_\alpha(t')\Big]\Big\},\end{aligned} \tag{4.75}$$

and we are now in the position to determine the order of magnitude of (4.75). As stated above, τ_R is assumed to be the characteristic decay time of $C_{\alpha\beta}(\tau)$, (4.70). Since the involved operators R_α and ρ_R are of $O(1)$, one can estimate

$$\int_0^{\infty} d\tau\ C_{\alpha\beta}(\tau) \sim \tau_R. \tag{4.76}$$

Since also the $S_\alpha \sim O(1)$ we can estimate

$$\frac{1}{T_S} \sim \frac{|\Delta\bar{\rho}_S|}{\Delta t}\frac{1}{|\bar{\rho}_S|} \sim \tau_R v^2. \tag{4.77}$$

The two conditions (4.68) and (4.71) become

$$\tau_R \ll \Delta t \ll \frac{1}{\tau_R v^2}, \tag{4.78}$$

which brings us to the necessary condition

$$\tau_R\, v \ll 1. \tag{4.79}$$

In terms of energy scales (4.78) reads

$$W_R \equiv \frac{1}{\tau_R} \gg \frac{1}{\Delta t} \gg v^2\tau_R \equiv \Gamma_S = \frac{1}{T_S}. \tag{4.80}$$

Here, W_R is the typical energy scale of the reservoir controlling its relaxation rate, e.g. the bandwidth or chemical potential μ, and Γ_S is a measure for the system-reservoir coupling which will be related to the system's relaxation rate. From (4.79) we have the requirement

$$W_R \gg v. \tag{4.81}$$

A further scale is the typical spacing $\Delta\varepsilon_S$ of the system's energies. Depending on its magnitude there can be two situations

(1) $\Delta\varepsilon_S \gg \Gamma_S \rightarrow$ *weak coupling* limit: One then takes

$$\Delta\varepsilon_S \gg \frac{1}{\Delta t} \gg \Gamma_S\,, \tag{4.82}$$

which leads to the so-called secular approximation, [83] which we are not going to discuss here.

(2) $W_R \gg \Delta\varepsilon_S \rightarrow$ *singular coupling* limit: Formally this is obtained by rewriting (4.51) as

$$H = H_S + \frac{1}{\delta}V + \frac{1}{\delta^2}H_R, \tag{4.83}$$

and taking $\delta \rightarrow 0$.

Of course one can, in principle, have both situations at the same time, provided

$$W_R \gg \Delta\varepsilon_S \gg \frac{1}{\Delta t} \gg \Gamma_S. \tag{4.84}$$

In these lectures we focus on the second case. The interesting situation is especially when $\Gamma_S \sim \Delta\varepsilon_S$, so that the action of the environment on the system cannot be regarded as small. Here we have

$$\frac{1}{\tau_R} \equiv W_R \gg \frac{1}{\Delta t} \gg \Delta\varepsilon_S \sim \Gamma_S. \tag{4.85}$$

We now return to the evolution equation for $\bar{\rho}_S(t)$, (4.75). Let us consider the eigenvectors $|n\rangle$ with eigenvalues ε_n of the system Hamiltonian in terms of which the time dependence of the system operators can be rewritten as

$$S_\alpha(t') = \sum_{m,n} |n\rangle\langle m|\langle n|S_\alpha|m\rangle e^{i(\varepsilon_n-\varepsilon_m)t'}, \tag{4.86}$$

see also (4.59). The integration in (4.75) has to be evaluated in the range $\tau \in (0, \tau_R)$ and $t' - t \in (0, \Delta t)$, which allows one to approximate

$$(\varepsilon_n - \varepsilon_m)t' \sim (\varepsilon_n - \varepsilon_m)(t' - \tau) \sim (\varepsilon_n - \varepsilon_m)t, \tag{4.87}$$

since $\Delta\varepsilon_S\ \Delta t \ll 1$ due to (4.85). Therefore, the detailed t'- and τ-dependence of S_α can be neglected and we can replace $S_\alpha(t')$ and $S_\alpha(t' - \tau)$ in (4.75) by $S_\alpha(t)$. This allows us to pull out the t-dependent terms and the integration $\frac{1}{\Delta t}\int_t^{t+\Delta t} dt' \to 1$ can be dropped. We denote the remaining integrals over the reservoir correlation functions by

$$C^{\pm}_{\alpha\beta} \equiv \int_0^\infty C_{\alpha\beta}(\pm\tau)\mathrm{d}\tau. \tag{4.88}$$

Furthermore, one can formally interpret $\Delta\bar{\rho}_S/\Delta t$ on the lhs of (4.75) as a derivative $\mathrm{d}\bar{\rho}_S/\mathrm{d}t$. The t-dependent terms in (4.75) are of the form

$$\begin{aligned} S_\alpha(t)S_\beta(t)\bar{\rho}_S(t) &= \underbrace{e^{iH_St}S_\alpha e^{-iH_St}}_{S_\alpha(t)} e^{iH_St}S_\beta \underbrace{e^{-iH_St}\bar{\rho}_S(t)e^{iH_St}}_{\rho_S(t)} e^{-iH_St} \\ &= e^{iH_St}S_\alpha S_\beta \rho_S(t)e^{-iH_St}. \end{aligned} \tag{4.89}$$

We now transform the derivative from the interaction to the Schrödinger representation. From differentiating

$$\bar{\rho}_S(t) = e^{iH_St}\rho_S(t)e^{-iH_St}, \tag{4.90}$$

one finds

$$\frac{\mathrm{d}\bar{\rho}_S(t)}{\mathrm{d}t} = e^{iH_S t}\left(i\left[H_S, \rho_S\right] + \frac{\mathrm{d}\rho_S}{\mathrm{d}t}\right)e^{-iH_S t}, \tag{4.91}$$

$$\Rightarrow \frac{\mathrm{d}\rho_S}{\mathrm{d}t} = -i\left[H_S, \rho_S\right] + e^{-iH_S t}\frac{\mathrm{d}\bar{\rho}_S(t)}{\mathrm{d}t}e^{iH_S t}, \tag{4.92}$$

where we omitted the time argument of $\rho_S(t)$, and the terms $e^{-iH_S t}\ldots e^{iH_S t}$ cancel the ones $e^{iH_S t}\ldots e^{-iH_S t}$ in (4.89). We thus get from (4.75) and (4.92)

$$\frac{\mathrm{d}\rho_S}{\mathrm{d}t} = -i\left[H_S, \rho_S\right] - v^2\sum_{\alpha\beta}\left(C^{+}_{\alpha\beta}\left[S_\alpha, S_\beta\rho_S\right] + C^{-}_{\alpha\beta}\left[\rho_S S_\alpha, S_\beta\right]\right), \tag{4.93}$$

with $C^{\pm}_{\alpha\beta}$ given in (4.88). Furthermore, by defining

$$C_{\alpha\beta} \equiv C^{+}_{\alpha\beta} + C^{-}_{\alpha\beta} = \int_{-\infty}^{\infty} C_{\alpha\beta}(\tau)\mathrm{d}\tau \tag{4.94}$$

$$\bar{C}_{\alpha\beta} \equiv C^{+}_{\alpha\beta} - C^{-}_{\alpha\beta} = \int_{-\infty}^{\infty} \mathrm{sgn}(\tau)C_{\alpha\beta}(\tau)\mathrm{d}\tau, \tag{4.95}$$

one arrives at

$$\begin{aligned}\frac{\mathrm{d}\rho_S}{\mathrm{d}t} =& -i\left[H_S, \rho_S\right] + v^2\sum_{\alpha,\beta}C_{\alpha\beta}\left(S_\beta\rho_S S_\alpha - \frac{1}{2}\{S_\alpha S_\beta, \rho_S\}\right)\\ &- v^2\sum_{\alpha,\beta}\bar{C}_{\alpha\beta}\frac{1}{2}\left[S_\alpha S_\beta, \rho_S\right].\end{aligned} \tag{4.96}$$

This expression can be rewritten in a more convenient form when explicitly considering that the coupling Hamiltonian V in (4.52) is Hermitian and, thus, can be rewritten as

$$V = v\sum_{\alpha} S_\alpha \otimes R_\alpha \tag{4.97}$$

$$= v\sum_{\alpha}{}' \left(S_\alpha \otimes R_\alpha + S^{\dagger}_{\alpha} \otimes R^{\dagger}_{\alpha}\right), \tag{4.98}$$

where the $\sum_{\alpha}{}'$ is such that the two expressions coincide. Introducing $\overline{\alpha}$ indices in such a way that

$$S_{\overline{\alpha}} = S^{\dagger}_{\alpha} \qquad R_{\overline{\alpha}} = R^{\dagger}_{\alpha}, \tag{4.99}$$

as well as new coefficients

$$\gamma_{\alpha\beta} \equiv C_{\overline{\alpha}\beta} v^2, \qquad i\sigma_{\alpha\beta} \equiv -v^2 \bar{C}_{\alpha\overline{\beta}}, \tag{4.100}$$

we can rewrite (4.96) as (we omit the prime from the sum from now on)

$$\begin{aligned} \frac{\mathrm{d}\rho_S}{\mathrm{d}t} &= -i\left[\widetilde{H}_S, \rho_S\right] + \sum_{\alpha\beta} \gamma_{\alpha\beta} \left(S_\beta \rho_S S_\alpha^\dagger - \frac{1}{2}\{S_\alpha^\dagger S_\beta, \rho_S\} \right) \\ &\equiv \mathcal{L}_H \rho_S + \mathcal{L}_D \rho_S . \end{aligned} \tag{4.101}$$

Here,

$$\widetilde{H}_S = H_S + \frac{1}{2} \sum_{\alpha\beta} \sigma_{\alpha\beta} S_\alpha S_\beta^\dagger . \tag{4.102}$$

Equation (4.101) is just the *Lindblad* equation (4.41) stated before, provided the coefficient matrix $\gamma_{\alpha\beta}$ is Hermitian and semipositive definite and $\sigma_{\alpha\beta}$ is Hermitian, which is straightforward to prove. As a side remark, the same form of the Lindblad equation is obtained in the weak-coupling limit (4.82), see, e.g. [83, 84, 87].

As mentioned before, $\mathcal{L} = \mathcal{L}_H + \mathcal{L}_D$ is the Lindblad superoperator. It consists of a unitary part $\mathcal{L}_H$, which simply provides a correction [the so-called "Lamb shift" cf. (4.102)] to the system Hamiltonian, and of the dissipator $\mathcal{L}_D$. Furthermore, notice that the Lindblad equation is Markovian since $\mathrm{d}\rho_S(t)/\mathrm{d}t$ only depends on $\rho_S(t)$, i.e. there are no contribution from the past values of $\rho_S(t)$.

4.4.4.3 Validity of Neglecting $\delta\bar{\rho}_{\mathrm{corr}}$

In order to derive the pleasant equation (4.101) we introduced the quite drastic approximation of neglecting correlations between system and environment described by $\delta\bar{\rho}_{\mathrm{corr}}$. Fortunately, one can readily show that this is justified without the need to introduce further assumptions beyond the ones we have already made in (4.85).

We follow the discussion of [88]. The correction term, as defined in (4.62), accounts for both correlations as well as changes in ρ_R. When including $\delta\bar{\rho}_{\mathrm{corr}}$ in (4.63), it enters in the first term on the r.h.s. and leads to the modification $\delta\Delta\bar{\rho}_S$, of $\Delta\bar{\rho}_S$:

$$\delta\Delta\bar{\rho}_S = -i\,\mathrm{Tr}_R \int_t^{t+\Delta t} \left[\bar{V}(t'), \delta\bar{\rho}_{\mathrm{corr}}(t)\right] \mathrm{d}t' . \tag{4.103}$$

Let us consider some initial time $t_0 < t$ at which $\delta\bar{\rho}_{\mathrm{corr}}(t_0) = 0$, e.g. $t_0 \to -\infty$. During the time evolution this term becomes nonzero due to V, and to first order in v we have

$$\delta\bar{\rho}_{\rm corr}(t) \sim \int_{-\infty}^{t} {\rm d}t''\,\bar{V}(t'')... \tag{4.104}$$

Upon insertion into (4.103) one finds terms of the form

$$\delta\Delta\bar{\rho}_S \sim \int_t^{t+\Delta t} {\rm d}t' \int_{-\infty}^{t} \underbrace{{\rm Tr}_R\left(\bar{V}(t')\bar{V}(t'')\rho_R\right)}_{v^2\langle R(t')R(t'')\rangle S(t')S(t'')} {\rm d}t''... \tag{4.105}$$

With (4.52) and (4.70) we can relate this to the reservoir correlation functions

$$v^2\langle R(t')R(t'')\rangle \sim C_{\alpha\beta}(t'-t'')v^2, \tag{4.106}$$

which are nonzero only in a small region $|t'-t''| < \tau_R$. This allows one to estimate

$$\delta\Delta\bar{\rho}_S \sim \int_t^{t+\tau_R} {\rm d}t' \int_{t-\tau_R}^{t} {\rm d}t'' C_{\alpha\beta}(t'-t'')v^2 \tag{4.107}$$

$$\sim v^2\tau_R^2\,, \tag{4.108}$$

which has to be compared with

$$\Delta\bar{\rho}_S \sim \frac{\Delta t}{T_S} \sim \Delta t\ \tau_R\ v^2. \tag{4.109}$$

Therefore, the condition for neglecting the contribution $\delta\Delta\bar{\rho}_S$ originating from δ becomes

$$\frac{\delta\Delta\bar{\rho}_S}{\Delta\bar{\rho}_S} \sim \frac{\tau_R}{\Delta t} \ll 1, \tag{4.110}$$

i.e. (4.71). In other words, averaging over a time $\Delta t \gg \tau_R$ allows one to "forget" the effects of correlations prior to t.

4.4.5 *Derivation for a Fermionic System-Reservoir Setup*

We now derive the Lindblad equation (4.48) from a microscopic fermion-reservoir model and discuss the limit in which the Lindblad representation of the reservoir becomes exact. According to (4.79) we need $W_R = \frac{1}{\tau_R} \gg v$, which is fulfilled when

(1) The DOS of the reservoir is ω-independent, i.e., the so-called *wide-band limit*

and

(2) T and/or $|\mu| \to \infty$, which corresponds to an ω-independent reservoir occupation.

We consider a generic noninteracting fermionic reservoir described by the Hamiltonian

$$H_R = \sum_k \varepsilon_k c_k^\dagger c_k,$$
$$V = \sum_{kn} v_{kn} \left(c_k^\dagger a_n + h.c. \right), \tag{4.111}$$

where $c_k^{(\dagger)}$ are reservoir and $a_n^{(\dagger)}$ system fermionic operators, and v_{kn} are real-valued coupling constants. We don't need to specify the form of the system Hamiltonian $H_S[a]$, since we just want to derive the effects of the reservoir. The reservoir levels ε_k must be continuous in order to produce dissipation, so we will let the level spacing go to zero, $\Delta\varepsilon \to 0$, and we introduce continuous operators[12]

$$c_k = \sqrt{\frac{\Delta\varepsilon}{2\pi}} c(\varepsilon)\,, \tag{4.112}$$

and couplings

$$v_{kn} = \sqrt{\frac{\Delta\varepsilon}{2\pi}} v_n(\varepsilon)\,, \tag{4.113}$$

where the system indices n remain discrete. In this way, the reservoir and coupling Hamiltonians become

$$H_R = \int \frac{\mathrm{d}\varepsilon}{2\pi}\, \varepsilon\, c^\dagger(\varepsilon) c(\varepsilon),$$
$$V = \sum_n \int \frac{\mathrm{d}\varepsilon}{2\pi}\, v_n(\varepsilon)\, c^\dagger(\varepsilon) a_n + h.c.$$
$$\equiv \sum_n R_n a_n + h.c. \tag{4.114}$$

This is in the form of (4.52), except for the fact that, for simplicity, we have absorbed v in the definition of the R_n. From (4.114) we read off

$$R_n = \int \frac{\mathrm{d}\varepsilon}{2\pi} v_n(\varepsilon) c^\dagger(\varepsilon), \tag{4.115}$$

We need to evaluate the reservoir correlation functions (4.70)

$$c_{\bar{n}m}(\tau) = \langle R_n^\dagger(\tau) R_m(0) \rangle, \tag{4.116}$$

[12] To be more rigorous: $c(\varepsilon) = \frac{1}{\sqrt{D(\varepsilon)}} \sum_k \delta(\varepsilon - \varepsilon_k) c_k$.

and

$$c_{n\bar{m}}(\tau) = \langle R_n(\tau) R_m^\dagger(0)\rangle = \int \frac{\mathrm{d}\varepsilon\, \mathrm{d}\varepsilon'}{(2\pi)^2}\, v_n(\varepsilon) v_m(\varepsilon') \langle c^\dagger(\varepsilon,\tau) c(\varepsilon')\rangle, \tag{4.117}$$

where

$$c^\dagger(\varepsilon,\tau) = e^{-i\varepsilon\tau} c^\dagger(\varepsilon)\,. \tag{4.118}$$

The occupation of reservoir states is given by

$$\langle c_k^\dagger c_{k'}\rangle = \delta_{kk'}\, n(k) = \frac{\Delta\varepsilon}{2\pi}\langle c^\dagger(\varepsilon) c(\varepsilon')\rangle, \tag{4.119}$$

and with $\delta_{kk'}/\Delta\varepsilon \to \delta(\varepsilon - \varepsilon')$ one finds that

$$\langle c^\dagger(\varepsilon,\tau) c(\varepsilon')\rangle = 2\pi\delta(\varepsilon-\varepsilon') n(\varepsilon) e^{-i\varepsilon\tau}\,, \tag{4.120}$$

by which (4.117) simplifies to

$$c_{n\bar{m}}(\tau) = \int \frac{\mathrm{d}\varepsilon}{2\pi}\, v_n(\varepsilon) v_m(\varepsilon)\, n(\varepsilon)\, e^{-i\varepsilon\tau}. \tag{4.121}$$

As discussed in (4.80), in order for the Lindblad equation representation of the reservoir to be accurate, the correlation functions (4.121) must decay fast enough, i.e. with a rate $1/\tau_R$ much larger than the $\Delta\varepsilon_S$ and v. $1/\tau_R$ is proportional to the width of the argument in (4.121), $F(\varepsilon) \equiv v_n(\varepsilon) v_m(\varepsilon) n(\varepsilon)$. Therefore, strictly speaking the Lindblad representation becomes exact when $F(\varepsilon)$ is constant. In this case,

$$c_{n\bar{m}}(\tau) \propto \delta(\tau)\,, \tag{4.122}$$

i.e. the Markovian condition. It is interesting to notice that this is the only requirement and once (4.122) is fulfilled there is no further weak-coupling requirement although a weak-coupling expansion was used for the Born-Markov approximation. The condition $F(\varepsilon) = $ const. requires both the wide-band limit $v_n(\varepsilon) = $ const. and $n(\varepsilon) = $ const.. The latter corresponds to having either (i) $\mu \to \pm\infty$ or (ii) $T \to \infty$. Otherwise, $c_{n\bar{m}}(\tau)$ decays with a rate $1/\tau_R$ proportional to the width of $F(\varepsilon)$. In nonequilibrium situations it is useful to have reservoirs with different occupations $n(\varepsilon)$. This is not in contradiction with the above condition since one can generalize (4.114) by including a sum over separate reservoirs α with constant but different occupations $n_\alpha(\varepsilon)$.

From (4.121) we determine the correlation functions (4.95), (4.100) by exploiting the following relations

$$I_1 \equiv \int_0^\infty e^{-i(\varepsilon - i\delta)\tau} \mathrm{d}\tau = \frac{1}{i(\varepsilon - i\delta)} = -i\mathrm{P}\frac{1}{\varepsilon} + \pi\delta(\varepsilon),$$
$$I_2 \equiv \int_{-\infty}^0 e^{-i(\varepsilon + i\delta)\tau} \mathrm{d}\tau = -\frac{1}{i(\varepsilon + i\delta)} = I_1^*. \tag{4.123}$$

This gives for the two matrices γ and σ of (4.101) and (4.102)

$$c_{n\bar{m}} = \int \mathrm{d}\tau\ c_{n\bar{m}}(\tau) = v_n(0)v_m(0)n(0) = \gamma_{\bar{n}\bar{m}},$$
$$\bar{c}_{n\bar{m}} = \int \mathrm{d}\tau\ c_{n\bar{m}}(\tau)\ \mathrm{sgn}(\tau) = -i\mathrm{P}\int \frac{\mathrm{d}\varepsilon}{\pi}\frac{1}{\varepsilon} v_n(\varepsilon)v_m(\varepsilon)n(\varepsilon) = -i\sigma_{nm}\,. \tag{4.124}$$

Even for energy independent $v_n(\varepsilon)v_m(\varepsilon)n(\varepsilon)$, the quantities σ_{nm} may be sensitive to their values at high energies. For simplicity, we here take even functions $v(\varepsilon)$, $n(\varepsilon)$, so that $\sigma_{nm} = 0$. Similarly

$$\gamma_{nm} = v_n(0)v_m(0)m(0) \qquad (m(\varepsilon) = 1 - n(\varepsilon)),$$
$$\sigma_{\bar{n}\bar{m}} = -\mathrm{P}\int \frac{\mathrm{d}\varepsilon}{\pi}\frac{1}{\varepsilon} v_n(\varepsilon)v_m(\varepsilon)m(\varepsilon)\ . \tag{4.125}$$

Thus, the parameters entering (4.48) are (we omit the ε-dependence of the v_n and of n)

$$2\Gamma_{1nm} = \gamma_{nm} = v_n v_m(1 - n),$$
$$2\Gamma_{2nm} = \gamma_{\bar{n}\bar{m}} = v_n v_m n. \tag{4.126}$$

As already discussed, Γ_{1nm} describes the removal of particles from the system which is consistent with it being proportional to $(1 - n)$, and Γ_{2nm} describes particle injection and is proportional to n.

For the 1-level model discussed above, we have in the steady state [cf. (4.50)]

$$\langle a^\dagger a\rangle = \frac{\Gamma_2}{\Gamma_1 + \Gamma_2} = n, \tag{4.127}$$

which we expect for a level in equilibrium with a reservoir.

4.5 Superfermion Representation

The so-called superfermion representation is a useful scheme to map the Lindblad equation onto a standard operator problem, in which the superoperator $\hat{\hat{\mathcal{L}}}$ acting on $\hat{\rho}$ is replaced by an ordinary operator $\hat{\mathcal{L}}$ acting on the corresponding state vector $|\rho\rangle$ in an enlarged Hilbert space. Like (4.42), the resulting equation is of "Schrödinger" type

$$\frac{\mathrm{d}}{\mathrm{d}t}|\rho\rangle = \hat{\mathcal{L}}|\rho\rangle, \tag{4.128}$$

in which, however, the "Hamiltonian" $i\hat{\mathcal{L}}$ is a non-Hermitian operator.

Here, we follow the treatment by Dzhioev and Kosov [65], see also [93, 94], as well as [66, 67] for an earlier treatment. The starting point is an augmented fermion Fock space, in which the original Hilbert space is doubled. Starting from the basis states $|n\rangle$ of the original space of dimension $N_{\mathcal{H}}$, one introduces additional"tilde" states and defines the new basis states $|n\rangle|\widetilde{m}\rangle$. The size of the new Hilbert space clearly becomes $N_{\mathcal{H}} \to N_{\mathcal{H}}^2$. This allows for a convenient representation of (system) density matrices[13]:

$$\hat{\rho} = \sum_{nm} |n\rangle \underbrace{\langle m|}_{\Rightarrow|\tilde{m}\rangle} \rho_{nm}. \tag{4.129}$$

For this one introduces the so-called "left vacuum"

$$|I\rangle = \sum_{m} |m\rangle|\widetilde{m}\rangle\,, \tag{4.130}$$

which is essentially a purification of the identity operator. Applying $\hat{\rho}$ to the left vacuum maps the density matrix onto a state vector of the augmented space.

$$\hat{\rho} \Rightarrow |\rho\rangle = \hat{\rho} \otimes \underbrace{\widetilde{I}}_{\text{implicit}} |I\rangle = \sum_{nm} \rho_{nm}|n\rangle|\widetilde{m}\rangle. \tag{4.131}$$

In general, for an arbitrary operator $\hat{B}$ one defines the corresponding state vector

$$|B\rangle \equiv \hat{B}|I\rangle\,, \tag{4.132}$$

which can be used to evaluate traces of operators

$$\mathrm{Tr}\hat{B} = \langle I|\hat{B}|I\rangle = \langle I|B\rangle. \tag{4.133}$$

[13] We omit here the system index of ρ_S for the sake of clarity.

Proof

$$\langle I|\hat{B}|I\rangle = \sum_{knm}\langle k|\langle\widetilde{k}|B_{nm}|n\rangle|\widetilde{m}\rangle = \sum_{k} B_{kk}. \tag{4.134}$$

In particular, expectation values of operators are given by

$$\begin{aligned}\langle\hat{A}\rangle = \mathrm{Tr}\hat{A}\hat{\rho} &= \langle I| \underbrace{\hat{A}\hat{\rho}}_{\text{(implicitly } \hat{A}\hat{\rho}\otimes\widetilde{I})} |I\rangle \\ &= \langle I|\hat{A}|\rho\rangle. \end{aligned}\tag{4.135}$$

Besides expressions of the form $\hat{A}\hat{\rho}$ we also need to evaluate $\hat{\rho}\hat{A}$, which occurs for instance in the Lindblad equation. For the first case we already found that $\hat{A}\hat{\rho} \to \hat{A}|\rho\rangle$ but a transformation of the form $\hat{\rho}\hat{A} \to \hat{\rho}\hat{A}|I\rangle$ is not useful, as we would like to express also the second case in terms of an operator applied to $|\rho\rangle$. $\hat{\rho}\hat{A}$ is written as

$$\hat{\rho}\hat{A} = \sum_{nm}\rho_{nm}|n\rangle\langle m|\hat{A}, \tag{4.136}$$

i.e. $\hat{A}$ acts on the bra vector $\langle m|$. Its representation within the augmented space is thus given by

$$\hat{\rho}\hat{A} \to \sum_{nm}(\hat{\rho}\hat{A})_{nm}|n\rangle|\widetilde{m}\rangle\ . \tag{4.137}$$

One now introduces the operator[14]

$$\widetilde{A} \equiv I\otimes A^T = \sum_{kl} A_{kl}|\widetilde{l}\rangle\langle\widetilde{k}|, \tag{4.138}$$

acting on tilde states only. Applied on the state $|\rho\rangle$ it provides the desired result

$$\begin{aligned}\widetilde{A}|\rho\rangle &= \sum_{klnm} A_{kl}|\widetilde{l}\rangle\langle\widetilde{k}|\rho_{nm}|n\rangle|\widetilde{m}\rangle \\ &= \sum_{lnm} A_{ml}\rho_{nm}|n\rangle|\widetilde{l}\rangle \\ &= \sum_{nl}(\hat{\rho}\hat{A})_{nl}|n\rangle|\widetilde{l}\rangle, \end{aligned}\tag{4.139}$$

which is the r.h.s. of (4.137), i.e. we have

$$\hat{\rho}\hat{A} \to \widetilde{A}|\rho\rangle. \tag{4.140}$$

[14]Note that the definition of A^T is basis dependent.

For a Fock space of fermionic particles one has to specify the fermionic sign of each term, or in other words the ordering of the levels when specifying states such as (4.130). Considering a many-fermion system characterized by levels $i = 1, 2, \ldots, N$, which may include spin, the basis states of the two Fock spaces are indicated as

$$\begin{aligned} |\underline{n}\rangle &= |n_1 n_2 \ldots n_N\rangle, \\ |\widetilde{\underline{n}}\rangle &\quad \text{“tilde” Fock space,} \end{aligned} \tag{4.141}$$

with corresponding creation and annihilation operators $a_i^\dagger$, a_i, $\widetilde{a}_i^\dagger$, $\widetilde{a}_i$. In the left vacuum one can include an arbitrary phase for each state. Here, it is convenient to adopt the convention

$$\begin{aligned} |I\rangle &= \sum_{\{\underline{n}\}} |\underline{n}, \widetilde{\underline{n}}\rangle, \\ |\underline{n}, \widetilde{\underline{n}}\rangle &= (-i)^{\sum_i n_i} (a_1^\dagger \widetilde{a}_1^\dagger)^{n_1} \ldots (a_N^\dagger \widetilde{a}_N^\dagger)^{n_N} \, |0\rangle|\widetilde{0}\rangle. \end{aligned} \tag{4.142}$$

Using this expression, one obtains the so-called *tilde conjugation rules* [65]:

$$\begin{aligned} a_j|I\rangle &= -i\,\widetilde{a}_j^\dagger|I\rangle, \\ a_j^\dagger|I\rangle &= -i\,\widetilde{a}_j|I\rangle. \end{aligned} \tag{4.143}$$

By taking their Hermitian conjugate, these can be easily generalized to

$$\begin{aligned} F|I\rangle &= -i\,\widetilde{F}^\dagger|I\rangle, \\ \langle I|F &= i\,\langle I|\widetilde{F}^\dagger, \end{aligned} \tag{4.144}$$

where F is an arbitrary linear combination of a_i, $a_j^\dagger$ with real coefficients.

Proof of (4.143):

$$\begin{aligned} a_j|I\rangle &= \sum_{\underline{n}:n_j=1} (-i)^{\sum_i n_i} \ldots a_j(a_j^\dagger \widetilde{a}_j^\dagger) \ldots |0\rangle|\widetilde{0}\rangle \\ &= -i\,\widetilde{a}_j^\dagger \sum_{\underline{n}:n_j=0} |\underline{n}, \widetilde{\underline{n}}\rangle \quad \text{(due to } \widetilde{a}_j^\dagger, n_j = 0 \text{ is guaranteed)} \\ &= -i\,\widetilde{a}_j^\dagger|I\rangle, \end{aligned}$$

and similarly for $a_j^\dagger$.

4.5.1 Representation of the Lindblad Equation

For a representation of the Lindblad equation (4.101), or specifically for fermions (4.48), we have to consider the representation of different operator terms multiplying the density matrix and applied to the left vacuum state. If the S_α are linear combinations of the $a_i^{(\dagger)}$ and a_i, we have for a quadratic term multiplied from the left

$$S_\alpha S_\beta \hat{\rho}|I\rangle = S_\alpha S_\beta |\rho\rangle, \tag{4.145}$$

and for one multiplied from the right

$$\hat{\rho} S_\alpha S_\beta |I\rangle = \hat{\rho} S_\alpha \underbrace{(-i\widetilde{S}_\beta^\dagger)}_{\substack{\text{can now be moved} \\ \text{to the left}}} |I\rangle \tag{4.146}$$

$$= i\widetilde{S}_\beta^\dagger \hat{\rho}(-i\widetilde{S}_\alpha^\dagger)|I\rangle \tag{4.147}$$

$$= \widetilde{S}_\beta^\dagger \widetilde{S}_\alpha^\dagger |\rho\rangle, \tag{4.148}$$

where we used (4.143). In a similar manner, quartic terms are transformed as

$$\hat{\rho} S_1 S_2 S_3 S_4 |I\rangle = \widetilde{S}_4^\dagger \widetilde{S}_3^\dagger \widetilde{S}_2^\dagger \widetilde{S}_1^\dagger |\rho\rangle, \tag{4.149}$$

and in general, for an operator O with an even number of fermionic a_i or $a_i^\dagger$ one has

$$\hat{\rho} O|I\rangle = \widetilde{O}^\dagger |\rho\rangle. \tag{4.150}$$

Finally, (4.101) contains terms with operators multiplying on the left and on the right that become[15]

$$S_\alpha \hat{\rho} S_\beta |I\rangle = -i\, S_\alpha \widetilde{S}_\beta^\dagger |\rho\rangle. \tag{4.151}$$

We are now in the position to express the superfermion representation of the Lindblad equation (4.101), or more specifically of $(\hat{\hat{\mathcal{L}}}\hat{\rho})|I\rangle$. The Liouville von Neumann part $\hat{\hat{\mathcal{L}}}_H$ becomes

$$\hat{\hat{\mathcal{L}}}_H \hat{\rho}|I\rangle = -i\left[H, \hat{\rho}\right]|I\rangle = -i\left(H - \widetilde{H}\right)|\rho\rangle, \tag{4.152}$$

i.e. we have the following mapping of the superoperator $\hat{\hat{\mathcal{L}}}_H$ in the superfermion space:

$$\hat{\hat{\mathcal{L}}}_H \Rightarrow -i\left(H - \widetilde{H}\right), \tag{4.153}$$

[15] Note that ρ contains even products of untilded fermion operators only, and thus commutes with tilde operators.

where $\widetilde{H}$ is the Hamiltonian applied to the "tilde" part of the Hilbert space [cf. (4.138)]. Here we used (4.150) and the fact that H is Hermitian and contains terms quadratic and quartic in the fermionic operators.

The dissipator $\hat{\hat{\mathcal{L}}}_D$ in (4.101) becomes

$$\left(\hat{\hat{\mathcal{L}}}_D\hat{\rho}\right)|I\rangle = \sum_{\alpha\beta}\gamma_{\alpha\beta}\left(-iS_\beta\widetilde{S}_\alpha - \frac{1}{2}S_\alpha^\dagger S_\beta - \frac{1}{2}\widetilde{S}_\beta^\dagger\widetilde{S}_\alpha\right)|\rho\rangle, \tag{4.154}$$

where we have used (4.145, 4.148, 4.151).

On the whole, (4.152) and (4.154) transform the Lindblad equation into a "Schrödinger-type" equation governing the time evolution of the "supervector" $|\rho\rangle$,

$$\frac{\mathrm{d}}{\mathrm{d}t}|\rho\rangle = \hat{\mathcal{L}}|\rho\rangle, \tag{4.155}$$

with a non-Hermitian generator $i\hat{\mathcal{L}}$. The trace preserving property of the Lindblad equation transforms into [cf. (4.133)]

$$\frac{\mathrm{d}}{\mathrm{d}t}\mathrm{Tr}\rho = 0 \quad \Rightarrow \quad \langle I|\frac{\mathrm{d}}{\mathrm{d}t}|\rho\rangle = \langle I|\hat{\mathcal{L}}|\rho\rangle = 0. \tag{4.156}$$

Since this holds true for any $|\rho\rangle$, one has

$$\langle I|\hat{\mathcal{L}} = 0. \tag{4.157}$$

Therefore, the left vacuum $\langle I|$ is a left eigenstate of $\hat{\mathcal{L}}$ with eigenvalue zero, which explains its name. For each left eigenstate there is a right one with the same eigenvalue. In this case this is the steady state $|\rho_\infty\rangle$ with the property

$$\hat{\mathcal{L}}|\rho_\infty\rangle = 0\,. \tag{4.158}$$

Equations of Motion

One way to address the time dependence of observables is via the *equations of motion* technique:

$$\begin{aligned}\langle A(t)\rangle &= \langle I|A|\rho(t)\rangle,\\ \frac{\mathrm{d}}{\mathrm{d}t}\langle A(t)\rangle &= \langle I|A\mathcal{L}|\rho(t)\rangle\\ &= \langle I|\underbrace{[A,\mathcal{L}]}_{\text{because }\langle I|\mathcal{L}=0}|\rho(t)\rangle.\end{aligned} \tag{4.159}$$

In some cases, e.g. noninteracting particles, this yields a closed set of equations. In the general interacting case, however, this is not possible and a hierarchy of equations is created, which must be truncated at some point. Below we discuss in more detail an alternative way, namely to directly solve (4.155) in a manybody basis.

Example (Single-level model) Consider again a fermionic system consisting of a single level with Hamiltonian (4.49) and dissipator (4.48) with no indices i, j. Using (4.154), the superfermion representation of the Lindblad operator becomes

$$\begin{aligned}\hat{\mathcal{L}} = &- i\varepsilon \left(a^\dagger a - \widetilde{a}^\dagger \widetilde{a}\right) - \Gamma_1 \left(a^\dagger a + \widetilde{a}^\dagger \widetilde{a} + 2ia\widetilde{a}\right) \\ &- \Gamma_2 \left(aa^\dagger + \widetilde{a}\widetilde{a}^\dagger + 2ia^\dagger \widetilde{a}^\dagger\right) \ ,\end{aligned} \tag{4.160}$$

which can be conveniently written in a matrix form

$$\begin{aligned}\hat{\mathcal{L}} &= -i \left(a^\dagger \widetilde{a}\right) \underline{\underline{H}} \begin{pmatrix} a \\ \widetilde{a}^\dagger \end{pmatrix} + \text{const.} \\ &= -i \underline{a}^\dagger \underline{\underline{H}}\, \underline{a},\end{aligned} \tag{4.161}$$

with the matrix $\underline{\underline{H}}$ given by

$$\underline{\underline{H}} = \begin{pmatrix} E_+ & B \\ \bar{B} & E_- \end{pmatrix} \qquad E_\pm = \varepsilon \pm i(\Gamma_2 - \Gamma_1),\ B = 2\Gamma_2,\ \bar{B} = -2\Gamma_1 \ . \tag{4.162}$$

We leave it as an exercise to use the equations of motion technique discussed above to evaluate the time dependence of the density

$$n(t) = \langle I | a^\dagger a | \rho(t) \rangle, \tag{4.163}$$

for this model.

Example (Current) Consider the single-level model (4.161), (4.162) coupled to two reservoirs, one described by the Γ_1 term and the other by the Γ_2 term only. Accordingly, we split the dissipator as

$$\mathcal{L}_D = \mathcal{L}_{D_1} + \mathcal{L}_{D_2}. \tag{4.164}$$

The current I_2 from the level to the Γ_2 reservoir is determined by the temporal change of the electron density in the level due to the coupling to the reservoir Γ_2 only:

$$I_2 = -\frac{\mathrm{d}}{\mathrm{d}t} \langle a^\dagger a \rangle_{\Gamma_2} \tag{4.165}$$

$$= -\mathrm{Tr} \left(a^\dagger a \hat{\hat{\mathcal{L}}}_{D_2} \rho \right) \tag{4.166}$$

$$= -\langle I | \left[a^\dagger a, \hat{\mathcal{L}}_{D_2} \right] | \rho \rangle. \tag{4.167}$$

We leave it as an exercise to determine the steady-state current and show that in steady state the current is conserved $I_1 = -I_2$.

4.5.1.1 Generic Fermionic Hamiltonian with Many Levels

For the case of a central system consisting of N noninteracting fermionic levels with Hamiltonian

$$H = \sum_{nm} \varepsilon_{nm} a_n^\dagger a_m,$$

and dissipator (4.48), it is straightforward to show that the expressions (4.161) with (4.162) still hold, provided one takes ε, Γ_1, Γ_2 as matrices with elements ε_{nm}, Γ_{1nm}, Γ_{2nm}, as well as

$$\underline{\underline{a}}^\dagger = \left(a_1^\dagger, \ldots, a_N^\dagger, \widetilde{a}_1, \ldots, \widetilde{a}_N\right). \tag{4.168}$$

If, additionally, an interaction described by a Hamiltonian H_U is present in the central system, the corresponding contribution to the Lindblad operator being $\hat{\hat{\mathcal{L}}}_U \hat{\rho} = -i\left[H_U, \hat{\rho}\right]$, becomes in the superfermion representation [cf. (4.153)]

$$\hat{\mathcal{L}}_U |\rho\rangle = -i(H_U - \widetilde{H}_U)|\rho\rangle. \tag{4.169}$$

Example (Anderson impurity chain attached to reservoirs) As a simple example, one can consider a fermionic tight-binding chain consisting of N sites (spin is not indicated explicitly) in which the leftmost site $n = 1$ is attached to a reservoir injecting particles, Γ_2 with the only nonzero matrix element $\Gamma_{2\,1,1}$, and the rightmost site $n = N$ is attached to a reservoir removing particles, Γ_1 with the only nonzero matrix element $\Gamma_{1\,N,N}$. One can include a Hubbard interaction U on the central chain, so that the system describes a nonequilibrium Anderson impurity chain in which a current flows from left to right, see upper part of Fig. 4.6. The corresponding superfermion Hamiltonian describes two chains, one corresponding to the operators a_n, the other to the $\widetilde{a}_n$. The two chains are coupled by the Γ and have opposite sign of the single-particle parameters. The Γ_2 (Γ_1) term injects (removes) particles on both chains, so that the total particle number is not conserved (see lower part of Fig. 4.6). However, if one carries out a particle-hole transformation for the tilde particles $\widetilde{d}_n = \widetilde{a}_n^\dagger$, then the total particle number $\sum_{n=1}^{N} \left(a_n^\dagger a_n + \widetilde{d}_n^\dagger \widetilde{d}_n\right)$ is conserved.

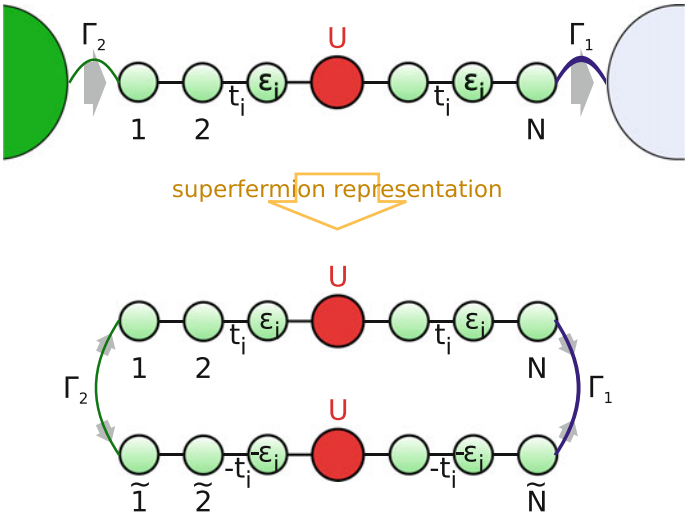

Fig. 4.6 (Top) Illustration of an Anderson impurity coupled to two reservoirs given by tight-binding chains with Lindblad drivings at the outermost sites. (Bottom) In the superfermion representation this maps onto to two chains, which are coupled via the Lindblad terms Γ_1 and Γ_2

4.6 Correlation Functions and Quantum Regression Theorem

Up to now we only discussed the time dependence of expectation values $\langle A(t)\rangle$. We now focus on two-time correlation functions $\langle A(t)B(t')\rangle$. The computation of such correlation or Green's functions is particularly important in the present treatment, since it enables us to combine the Lindblad approach with the framework of nonequilibrium Green's functions, as outlined below in more detail.

The time dependence of an operator A acting on the system only is given by

$$\langle A(t)\rangle = \mathrm{Tr} A(t)\varrho = \mathrm{Tr}_S \mathrm{Tr}_R A\varrho(t) = \mathrm{Tr}_S A\varrho_S(t), \tag{4.170}$$

with $\varrho_S = \mathrm{Tr}_R \varrho$ the system reduced and ϱ the universe density matrix. Here, we have exploited the fact that the Heisenberg time evolution of an operator A has opposite sign with respect to the time evolution of ρ, the cyclic property of the trace, and that the reservoir trace can be "pulled over" the system operator A. Due to this, it is sufficient to know the time dependence of $\varrho_S(t)$, which is given by the Lindblad equation (4.41) as discussed up to now. However, for two-time correlation functions of system operators a knowledge of $\varrho_S(t)$ is no longer sufficient. Let us illustrate this for the following correlation function of two system operators A, B:

$$
\begin{aligned}
iG_{BA}(t_1+\tau,t_1) &= \mathrm{Tr}B(t_1+\tau)A(t_1)\varrho \\
&= \mathrm{Tr}e^{iH(t_1+\tau)}Be^{-iH(t_1+\tau)}e^{iHt_1}Ae^{-iHt_1}\varrho \\
&= \mathrm{Tr}Be^{-iH\tau}A\varrho(t_1)e^{iH\tau} = \mathrm{Tr}_S\, B\,\mathrm{Tr}_R\, e^{-iH\tau}A\varrho(t_1)e^{iH\tau}. \qquad (4.171)
\end{aligned}
$$

Now, since the Hamiltonian H acts on both system and reservoir, one cannot pull Tr_R over $e^{-iH\tau}$.

In order to make progress, let us introduce the following system operator

$$
A_S(\tau,t_1) := \mathrm{Tr}_R\, e^{-iH\tau}A\varrho(t_1)e^{iH\tau}, \qquad (4.172)
$$

in terms of which

$$
iG_{BA}(t_1+\tau,t_1) = \mathrm{Tr}_S\, BA_S(\tau,t_1). \qquad (4.173)
$$

Unfortunately, $A_S(\tau,t_1)$ cannot be determined solely from the knowledge of the reduced density matrix $\varrho_S(t_1)$. Fortunately, the so-called *quantum regression theorem* [85, 87] states that the time dependence of the operator $A_S(\tau,t_1)$ is governed by an equation of Lindblad type

$$
\frac{d}{d\tau}A_S(\tau,t_1) = \underline{\mathcal{L}}A_S(\tau,t_1), \qquad (4.174)
$$

provided that the same Markovian conditions as for ρ_S, (4.80), hold true:

$$
T_S \gg \Delta t \gg \tau_R. \qquad (4.175)
$$

This result combined with the initial ($\tau = 0$) condition

$$
A_S(0,t_1) = \mathrm{Tr}_R\, A\varrho(t_1) = A\varrho_S(t_1), \qquad (4.176)
$$

allows to determine an arbitrary operator $A_S(\tau,t_1)$, and thus any two-time correlation function $iG_{BA}(t+\tau,t_1)$. This works as follows:

(1) First calculate $\rho_S(t_1)$ from $\frac{d}{dt_1}\rho_S = \mathcal{L}\rho_S$ and a given initial condition. In particular, we are interested in the steady state case $t_1 \to \infty$, see below.
(2) Then compute the τ-time evolution of $A_S(\tau,t_1)$ from (4.174), with initial condition (4.176), taking t_1 as a fixed parameter.

In fact, for the case that A is a bosonic operator (or contains even products of fermionic creation/annihilation operators), $\underline{\mathcal{L}}$ and $\mathcal{L}$ from (4.41) coincide. For the case of operators containing odd products of fermions, which is relevant in evaluating single-particle Green's functions, there is an additional sign, [95], which we are going to discuss below.

The Quantum Regression Theorem (4.174) can be readily proven by repeating the steps of Sect. 4.4.4 whereby one takes instead of the universe density matrix $\rho(t)$, the quantity $[A\varrho(t_1)](t)$, where $\frac{d}{dt}[\cdots](t) = -i[H,[\cdots](t)]$, c.f. (4.53). Since the

quantity we are looking for is precisely $A_S(t,t_1) = \mathrm{Tr}_R[A\varrho(t_1)](t)$ (cf. (4.172)), the procedure carried out to determine the time dependence of $\rho_S(t)$ ((4.54)) is precisely the same. As a result, one gets the same (4.174) with $\underline{\mathcal{L}} = \mathcal{L}$. For fermions, one should take care of the fact that the coupling Hamiltonian cannot be readily written in the form (4.52), since there are additional fermionic signs. In the end, this leads to a slightly different expression for $\underline{\mathcal{L}}$, which we are going to discuss below. See [95], Appendix B, for a complete treatment.

One should point out that the Lindblad time evolutions (4.174) and (4.41) are valid only in the positive direction of time. Inherently, this is connected to the Markov approximation and the dissipative dynamics. However, in the case of correlation functions we generally need to compute $iG_{BA}(t+\tau,t)$ for $\tau < 0$ as well. This can be achieved in two ways

- Instead of $iG_{BA}(t+\tau,t)$ one considers the complex conjugate

$$\begin{aligned} -iG^*_{BA}(t+\tau,t) &= \mathrm{Tr}A^\dagger(t)B^\dagger(t+\tau)\varrho \\ &= iG_{A^\dagger B^\dagger}(t,t+\tau), \end{aligned} \tag{4.177}$$

  which is in the proper time order since $t-(t+\tau) > 0$ for $\tau < 0$.
- Alternatively, with the cyclic invariance of the trace one has that

$$\begin{aligned} iG_{BA}(t+\tau,t) &= \mathrm{Tr}A(t)\varrho B(t+\tau) \\ &= \mathrm{Tr}_S\, A\, \mathrm{Tr}_R\left\{e^{iH\tau}\varrho(t+\tau)Be^{-iH\tau}\right\} \\ &= \mathrm{Tr}_S\, A\widetilde{B}^\dagger_S(-\tau,t+\tau), \end{aligned} \tag{4.178}$$

  and the time evolution of $\widetilde{B}^\dagger_S(-\tau,t+\tau)$ is determined by (4.174) for $\tau < 0$.

4.6.1 Superfermion Representation

We now want to express a correlation function (4.173) in the superfermion formalism of Sect. 4.5. In this notation,

$$iG_{BA}(t_1+\tau,t_1) = \langle I|BA_S(\tau,t_1)|I\rangle \equiv \langle I|B|A_S(\tau,t_1)\rangle\rangle\ . \tag{4.179}$$

Here, the supervector $|A_S(\tau,t_1)\rangle\rangle$ has the properties

$$\frac{d}{d\tau}|A_S(\tau,t_1)\rangle\rangle = \hat{\mathcal{L}}|A_S(\tau,t_1)\rangle\rangle, \qquad |A_S(0,t_1)\rangle\rangle = A|\rho_S(t_1)\rangle\rangle, \tag{4.180}$$

provided A is a bosonic operator. This can be easily shown by using (4.174), (4.176), and (4.144), and proceeding like for (4.145, 4.148, 4.151). For fermionic operators the derivation is somewhat more tricky, but in the end one obtains effectively the

same expression (4.180) with the same $\hat{\mathcal{L}}$, despite of the fact that in (4.174) $\hat{\underline{\hat{\mathcal{L}}}}$ differs from $\hat{\hat{\mathcal{L}}}$. This is discussed in the next section.

Note that the expression (4.179) is valid for $\tau > 0$ only. For negative τ one should use (4.177) or (4.178).

4.6.2 Fermionic Operators

As mentioned above, special care has to be taken for the case of fermionic operators since their expression in terms of tensor products is not trivial. We here only sketch the issue and refer to [95], Appendix B, for a complete treatment. The system operator A of Sect. 4.6 has in fact the form $A = I_R \otimes A_S$. On the other hand, a single-particle fermionic operator C for the system does not have this form since it anti-commutes with reservoir states. Consider for instance the product state $|\psi\rangle = |R\rangle \otimes |S\rangle$. Here,[16]

$$C|\psi\rangle = (-1)^{N_R}|R\rangle \otimes C_S|S\rangle\,, \tag{4.181}$$

with N_R the number of fermions in state $|R\rangle$. Therefore, one must include these phase factors in the definition of the tensor product operators, leading to

$$C = (-1)^{N_R} \otimes C_S. \tag{4.182}$$

When carrying out the microscopic derivation of Sect. 4.4.4, one finds that these sign factors cancel away in the case of the Lindblad equation for the density matrix ρ, while for correlation functions they do matter.

Following the treatment of [95], Appendix B, one obtains that a fermionic operator $C_S(\tau, t_1)$ defined similarly to (4.172) obeys

$$\frac{d}{d\tau}C_S(\tau, t_1) = \hat{\underline{\hat{\mathcal{L}}}}C_S(\tau, t_1)\,, \tag{4.183}$$

with

$$\hat{\underline{\hat{\mathcal{L}}}}C_S := -i\,[H, C_S] + \sum_{\alpha\beta}\gamma_{\alpha\beta}\left(\eta S_\alpha C_S S_\beta^\dagger - \frac{1}{2}\left\{S_\beta^\dagger S_\alpha, C_S\right\}\right). \tag{4.184}$$

The additional sign factor η (possibly) distinguishes this result from (4.41) and is equal to -1 if C_S and S_α both contain an odd number of fermionic operators, and $+1$ otherwise.

[16] C_S is the same as C but acting on the system Hilbert space only.

Nevertheless, the pleasant aspect is that in the superfermion representation of Sect. 4.5, this sign η cancels out again. Therefore, in the superfermion representation, the vector $|C_S(\tau, t_1)\rangle$ associated to $C_S(\tau, t_1)$ obeys an equation like (4.155)

$$\frac{d}{d\tau}|C_S(\tau, t_1)\rangle = \hat{\mathcal{L}}|C_S(\tau, t_1)\rangle, \tag{4.185}$$

with the same $\hat{\mathcal{L}}$ (4.153), (4.154).

4.7 Nonequilibrium Green's Functions

Nonequilibrium Green's functions have been treated in detail in the previous two lectures, so here we are simply going to summarize the parts which are most relevant for the present treatment. Again we specialize to the case of a fermionic system. We refer to these lectures and to previous literature (see, e.g. [1, 2, 96]).

As introduced by Kadanoff, Baym and Keldysh, a modified time contour ordering allows one to formulate a systematic Green's function formalism analogous to the equilibrium case. In contrast to equilibrium, the system states at $t \to \pm\infty$ are no longer equivalent and thus the only reference point is the infinite past.[17] Only there one can assume that the system is in a noninteracting initial state necessary in order to apply Wick's theorem. Therefore, instead of time-ordered expectation values as in equilibrium, one has to consider contour-ordered ones. Different contour orders exist and we focus here only on the Keldysh contour, as sketched in Fig. 4.7. Here, the Matsubara branch, accounting for initial correlations, is neglected and the contour extends until $t \to -\infty$. This is justified when considering steady states or even when carrying out time evolutions starting from a steady state.[18] An example for a two-time correlation function is depicted in Fig. 4.7, which demonstrates that the contour-ordering of times generally differs from the ordinary time-ordering. When denoting contour times by $\tau_{A/B}$ and "standard" times by $t_{A/B}$, one can write contour-ordered two-time Green's functions in the following way

$$G(\tau_A, \tau_B) \Rightarrow \hat{G}(t_A, t_B) = \begin{pmatrix} G_T(t_A, t_B) & G^<(t_A, t_B) \\ G^>(t_A, t_B) & G_{\bar{T}}(t_A, t_B) \end{pmatrix}. \tag{4.186}$$

It is convenient to employ a matrix structure, which contains all the possible orderings of the two time variables $t_{A/B}$ on the lower and on the upper contour. $G_T(t_A, t_B)$ ($G_{\bar{T}}(t_A, t_B)$) is the time (anti-time) ordered Green's function, which corresponds to the case that t_A and t_B are both on the upper (lower) contour. The lesser (greater)

[17] In case of the L-shaped Kadanoff-Baym contour this starting point is on the imaginary-time Matsubara branch, i.e. corresponds to a thermal initial state.

[18] In principle, one could avoid the Matsubara branch altogether by designing a Hamiltonian whose steady state is the required initial state.

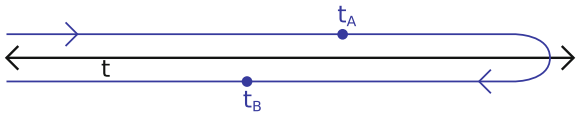

Fig. 4.7 Sketch of the Keldysh contour with an upper and a lower branch, both extending to $-\infty$. Depicted is the example of a "lesser" two-time function (e.g. $G^<(t_A, t_B)$), in which t_A is before t_B in terms of the contour ordering

Green's function $G^<(t_A, t_B)$ ($G^>(t_A, t_B)$) refers to the mixed cases, with one time variable on the upper and one on the lower time contour.

The matrix form stated above contains redundant information and it is thus convenient to employ a transformation [2]

$$\underline{G} = L\sigma_3\hat{G}L^\dagger = \begin{pmatrix} G_R & G_K \\ 0 & G_A \end{pmatrix}, \tag{4.187}$$

to the so-called Keldysh space. The retarded (G_R), advanced (G_A) and Keldysh (G_K) Green's functions are hereby defined as:

$$\begin{aligned} G_R(1,2) &= -i\Theta(t_1 - t_2)\langle\{c(1), c^\dagger(2)\}\rangle, \\ G_A(1,2) &= G_R(2,1)^\dagger, \\ G_K(1,2) &= -i\langle[c(1), c^\dagger(2)]\rangle. \end{aligned} \tag{4.188}$$

The matrix form (4.187), which we shall indicate by an underscore "_", is very useful since essentially the full perturbation theory and Feynman diagrams developed for equilibrium is also applicable in the nonequilibrium case, whereby all scalar expressions for the Green's functions have to replaced by analogous matrix expressions.

Besides matrix products, one also needs to compute inverses $\underline{F}^{-1}$ of two-point Keldysh objects $\underline{F}$. This is given in terms of the Langreth rules, by

$$\underline{F} = \begin{pmatrix} F_R & F_K \\ 0 & F_A \end{pmatrix} \quad \rightarrow \quad \underline{F}^{-1} = \begin{pmatrix} F_R^{-1} & -F_R^{-1}F_K F_A^{-1} \\ 0 & F_A^{-1} \end{pmatrix}, \tag{4.189}$$

whereby the individual objects $F_R, F_K, \ldots$ can also be matrices in site and/or spin indices. Clearly, retarded objects transform in a simple manner and only the Keldysh part is more involved

$$\begin{aligned} (\underline{F}^{-1})_R &= (F_R)^{-1}, \\ (\underline{F}^{-1})_K &= -F_R^{-1}F_K F_A^{-1}. \end{aligned} \tag{4.190}$$

4.7.1 Anderson Impurity Model

As mentioned at the beginning, we are particularly interested in the nonequilibrium Anderson impurity model, which is described by the Hamiltonian

$$\begin{aligned} H &= H_C + H_R + V, \\ H_C &= \varepsilon \sum_\sigma c_{0\sigma}^\dagger c_{0\sigma} + U n_{0\uparrow} n_{0\downarrow}, \\ H_R &= \sum_{\sigma, p\neq 0} \varepsilon_p c_{p\sigma}^\dagger c_{p\sigma}, \\ V &= \sum_{\sigma, p\neq 0} v_p c_{p\sigma}^\dagger c_{0\sigma} + \text{h.c.}, \end{aligned} \tag{4.191}$$

with H_C the impurity, H_R the reservoir and V the coupling Hamiltonian.[19] For the reservoir we consider the case of two leads denoted by $+$ and $-$, corresponding to $p > 0$ and $p < 0$ in (4.191), with different chemical potentials (μ_+, μ_-) and temperatures (T_+, T_-), see left side of Fig. 4.8. The unperturbed Hamiltonian

$$H_0 = H_- + H_+ + H_{C0}. \tag{4.192}$$

corresponds to the decoupled system without interaction and we consider as perturbation the hybridizations v_p and the interaction U. At $t_0 \to -\infty$ the system is prepared in an eigenstate of H_0, i.e. the three regions are separately in equilibrium with their respective chemical potentials and temperatures, and the perturbation is then switched on. For $t - t_0 \to \infty$ the system reaches the steady state of the full Hamiltonian (4.191). In the steady state one can assume that time translational invariance applies, so that Green's functions can be written in the frequency domain:

$$\underline{G}(t_1 - t_2) \to \underline{G}(\omega)\,. \tag{4.193}$$

From now on we assume that all Green's functions are ω-dependent and omit the argument for the sake of simplicity.

Let us start with the noninteracting case $U = 0$, so that the perturbation is only given by the hybridizations to the leads. For this case the exact Dyson equation reads

$$\underline{G} = \underline{g} + \underline{g}\,\underline{V}\,\underline{G}. \tag{4.194}$$

The equation is analogous to the equilibrium case, the difference being that every object has a 2×2 matrix structure in Keldysh space, in addition to level and/or

[19] Similarly, one could also generalize the steps outlined below to the situation of a central system containing a small number of interacting sites, see Fig. 4.1, by a suitable matrix notation.

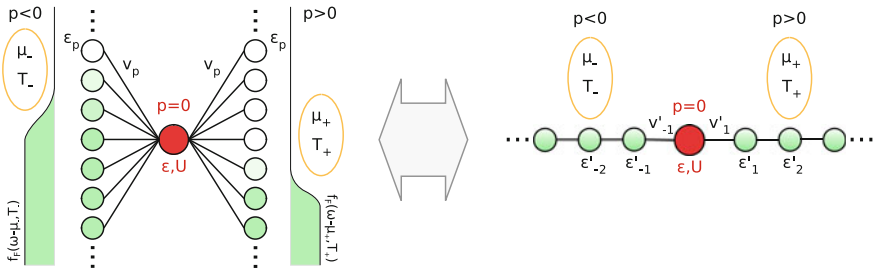

Fig. 4.8 (Left) Sketch of the nonequilibrium Anderson impurity model as defined in (4.191). The two reservoirs $p < 0$ and $p > 0$ consist of an infinite number of levels ε_p, which are (at $t_0 \to -\infty$) filled according to the Fermi-Dirac distributions $f_F(\omega - \mu_\pm, T_\pm)$. This is the "star" representation. (Right) Equivalent "chain" representation, with two semi-infinite chains representing the reservoirs

spin indices. $\underline{G}$ is the full Green's function, $\underline{g}$ is the Green's function of the isolated regions ($v_p = 0$) and $\underline{V}$ is the hybridization, which is diagonal in Keldysh space:

$$\underline{V}_{0p} = \underline{V}_{p0} = \begin{pmatrix} v_p & 0 \\ 0 & v_p \end{pmatrix}. \tag{4.195}$$

In principle, the full matrices in (4.194) can be inverted with the help of (4.189). It is convenient to write them explicitly in terms of their components

$$\begin{aligned} \underline{G}_{00} &= \underline{g}_{00} + \underline{g}_{00} \sum_p \underline{V}_{0p} \underline{G}_{p0}, \\ \underline{G}_{p0} &= \underbrace{\underline{g}_{p0}}_{0} + \sum_{p'} \underline{g}_{pp'} \underline{V}_{p'0} \underline{G}_{00}. \end{aligned} \tag{4.196}$$

Here, we made use of the fact that $\underline{g}_{pp'}$ does not have off-diagonal components linking the initially decoupled regions. On the whole, one can write Dyson's equation as

$$\underline{G}_{00} = \underline{g}_{00} + \underline{g}_{00}\, \underline{\Delta}\, \underline{G}_{00}, \tag{4.197}$$

with the bath *hybridization function* defined as

$$\underline{\Delta} = \sum_{p,p'} \underline{V}_{0p} \underline{g}_{pp'} \underline{V}_{p'0}\,. \tag{4.198}$$

As usual, the solution of (4.197) is obtained by

$$\underline{G}_{00} = \left(\underline{g}_{00}^{-1} - \underline{\Delta} \right)^{-1}, \tag{4.199}$$

whereby one has to take the Langreth rules (4.189) into account, in order to invert the 2×2 Keldysh objects.

The reservoir Green's functions $\underline{g}_{pp'}$ are known analytically, since they correspond to a noninteracting system in equilibrium.[20] For a reservoir Hamiltonian as specified in (4.191), which is diagonal in the p operators, the retarded part is given by

$$g_{Rpp'}(\omega) = \delta_{pp'} \left(\omega - \varepsilon_p + i0^+\right)^{-1} . \tag{4.200}$$

Of course, other choices of the reservoir are possible as well, e.g. a "chain" instead of a "star" representation, see Fig. 4.8. In the latter case, only one site of each lead, e.g. $g_{R11}(\omega)$ and $g_{R-1-1}(\omega)$, would couple to the central system. Notice that such "surface" Green's function of a noninteracting semi-infinite tight-binding chain can be determined analytically, cf. [97].

In equilibrium, the Keldysh and the retarded Green's functions are not independent but linked via the so-called *fluctuation dissipation theorem*:

$$\begin{aligned} g_{Kpp}(\omega) &= \left(g_{Rpp}(\omega) - g_{App}(\omega)\right) s_p(\omega), \\ s_p(\omega) &= 1 - 2f_F(\omega - \mu_p, T_p), \end{aligned} \tag{4.201}$$

with $f_F(\omega - \mu_p, T_p)$ the Fermi-Dirac distribution. For the nonequilibrium case, the Keldysh and the retarded component are independent functions and both of them must be considered explicitly.

As in equilibrium, the solution of the interacting problem $U \neq 0$ poses the main challenge. A couple of different approaches are discussed in the next section. Here, let us focus on the general properties. As usual, the contribution from U can be encoded in terms of the self energy $\underline{\Sigma}(\omega)$, which is also a 2×2 Keldysh object in nonequilibrium. In terms of site indices pp', $\underline{\Sigma}(\omega)$ is only nonzero when an interaction term is present in the Hamiltonian at p and p'. Therefore, in the single impurity case considered here, the self energy has only contributions on the impurity site. In this way, (4.199) is modified to

$$\underline{G}_{00} = \left(\underline{g}_{00}^{-1} - \underline{\Delta} - \underline{\Sigma}_{00}\right)^{-1} . \tag{4.202}$$

Once $\underline{\Sigma}_{00}$ is known, all single particle quantities of interest can be computed.[21] The possibly spin-dependent particle density on the impurity site, for instance, is given in terms of the Keldysh Green's function by

$$n = \frac{1}{2} - \frac{i}{4\pi} \int G_{K00}(\omega) \mathrm{d}\omega . \tag{4.203}$$

[20] Note that $\underline{g}$ refers to the initially decoupled situation.

[21] We focus here on the impurity, but also reservoir properties are accessible via Dyson's equation.

The current from the reservoir to the impurity is determined in terms of G_{Kp0} leading to the Meir-Wingreen formula: [98]

$$j = \frac{i}{2\pi}\int_{-\infty}^{\infty} \mathrm{d}\omega \left(\left[\gamma_-(\omega) - \gamma_+(\omega)\right] G^<_{00}(\omega) + \left[f_{F-}(\omega)\gamma_-(\omega) - f_{F+}(\omega)\gamma_+(\omega)\right] \left[G_{R00}(\omega) - G_{A00}(\omega)\right] \right), \quad (4.204)$$

with $f_{F\pm}$ the Fermi functions of the left (-) and right (+) reservoir, and $\gamma_\pm(\omega) = -2\Im\mathrm{m}\left\{\Delta_{R\pm}(\omega)\right\}$ accounts for the coupling strength to and the DOS of each lead.

4.8 Nonequilibrium Impurity Problems

The manybody solution of nonequilibrium impurity problems, as defined by (4.191), is an active area of research and numerous different approaches were devised in recent years. Here, we want to give only a brief overview over some of them and then focus on solution strategies based on a combination of nonequilibrium Green's functions and Lindblad equations, which is the topic of the present lecture.

Powerful numerical methods for the solution of equilibrium impurity models are for instance exact diagonalization (ED), quantum Monte Carlo (QMC), matrix product states (MPS) and numerical renormalization group (NRG). Except for action-based QMC solvers, the common solution strategy is to replace the exact hybridization function $\underline{\Delta}(\omega)$ by an approximate one, corresponding to a finite size system which can be solved precisely by numerical techniques (see, e.g., Fig. 4.9).

The key point is always that the influence of the leads is completely determined by $\underline{\Delta}(\omega)$. In other words, the self energy $\underline{\Sigma}(\omega)$ depends solely on ε, U and $\underline{\Delta}(\omega)$, but not on other details of the reservoir. This means that different representations of the reservoir, for instance a chain or a star geometry, which yield the same $\underline{\Delta}(\omega)$ are equivalent on the level of impurity properties. Both of them result in the same $\underline{G}_{00}$

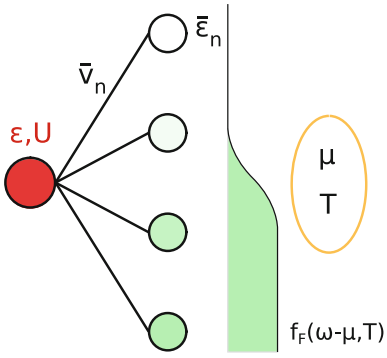

Fig. 4.9 Exact diagonalization approach as used for equilibrium situations. Instead of the exact system, Fig. 4.8 with a single reservoir, e.g. $p > 0$ only, a finite size problem consisting of the impurity and a small number of levels $\bar{\varepsilon}_n$ is solved

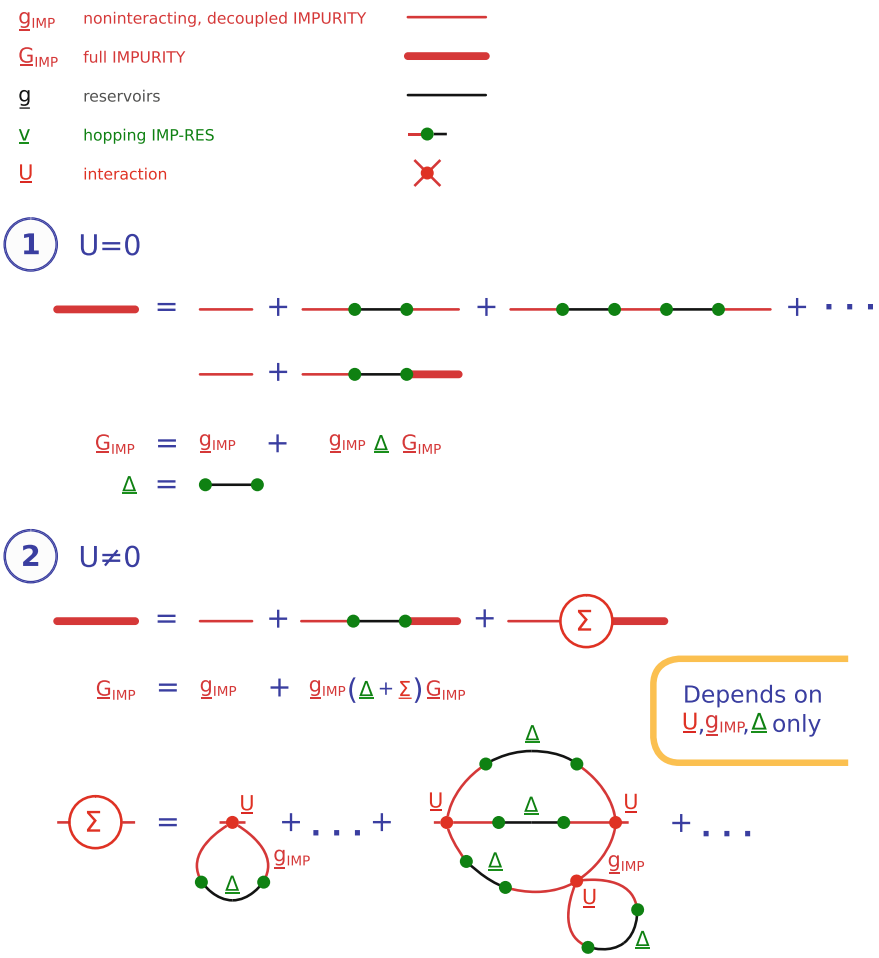

Fig. 4.10 Sketch of the diagrammatic proof that correlation functions on the impurity site are fully determined by the hybridization function $\underline{\Delta}(\omega)$, and the impurity terms U and $\underline{g}_{\rm IMP}$. Other details of the bath are irrelevant, e.g. whether one considers a "star" or "chain" representation, cf. Fig. 4.8. The bath can be also represented by a mixed auxiliary system consisting of orbitals and Lindblad terms, such as a buffer layer (see Sect. 4.8.1) or by a more generic one within the Auxiliary Master Equation Approach [21, 63], as depicted in Fig. 4.13, see Sect. 4.9

and $\underline{\Sigma}_{00}$. Of course, this fact holds in nonequilibrium as well, see Fig. 4.10. Within NRG, this fact is exploited to justify the Wilson chain [6].

In equilibrium one exploits this to replace the dense reservoir by an auxiliary reservoir with a small number of levels only and different parameters $\bar{\varepsilon}_n$, $\bar{v}_n$, see Fig. 4.9. Here, the parameters are determined (fitted) in order to provide the best representation of the bath hybridization function $\Delta(i\omega_\lambda)$ in Matsubara frequency space. This is the exact-diagonalization based impurity solver [8, 9], widely used for DMFT.

Out of equilibrium this does not work since a finite size reservoir cannot provide dissipation and thus a steady state situation can never be reached in the time evolution. Instead, such a system exhibits oscillating dynamics. Here, we want to consider closely related approaches, in which the reservoir is modeled by a small number of levels which are additionally coupled to Markovian environments. Such auxiliary systems are governed by a Lindblad equation, which we discussed earlier. The key advantage is that these reservoir representations exhibit dissipative dynamics and truly represent nonequilibrium impurity systems.

4.8.1 Buffer Layer Approach

In the so-called buffer layer approach, see e.g. [65], one considers a certain number N_B of bath levels coupled to the impurity site, similar to the original Hamiltonian (4.191) but with N_B finite. To "compensate" for the missing part of the infinite reservoir one additionally couples the bath sites to Markovian environments, see also Fig. 4.11. In this way one is able to achieve a continuous DOS in the auxiliary system, appropriate for a nonequilibrium situation.

If one assumes for the Markovian environments an infinite bandwidth and energy-independent occupations n_n, the auxiliary system can be exactly written in terms of a Lindblad equation, as previously discussed

$$\dot{\rho} = \mathcal{L}_H \rho + \mathcal{L}_D \rho,$$
$$\mathcal{L}_D \rho = 2 \sum_{n=1}^{N_B} \left(\Gamma_{1n} \left(d_n \rho d_n^\dagger - \frac{1}{2} \{ d_n^\dagger d_n, \rho \} \right) + \Gamma_{2n} \left(d_n^\dagger \rho d_n - \frac{1}{2} \{ d_n d_n^\dagger, \rho \} \right) \right), \quad (4.205)$$

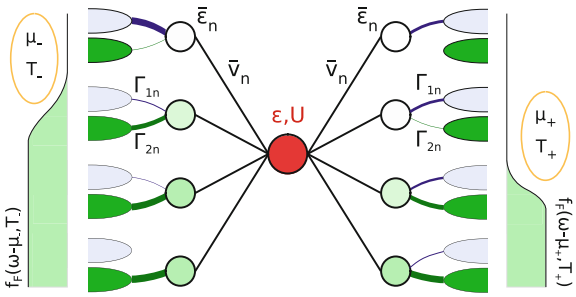

Fig. 4.11 Buffer layer approach: The nonequilibrium impurity model Fig. 4.8 is replaced by a finite number of levels $\bar{\varepsilon}_n$ which are additionally coupled to Markovian environments. The appropriate filling $n_n = f_F(\bar{\varepsilon}_n - \mu_\pm, T_\pm)$ is achieved by suitable coupling constants Γ_{1n} and Γ_{2n} to the empty and filled Markovian environments, (4.206). The resulting finite size open quantum system is governed by a Lindblad equation (4.205) and represents a true nonequilibrium model

where ρ represents the density matrix of the open system consisting of impurity plus level sites with corresponding operators d_n. There are two types of Markovian environments, one completely empty ($\mu \to -\infty$) and one completely filled ($\mu \to +\infty$). The coefficients Γ_{1n} determine the couplings to the empty environment, and Γ_{2n} the couplings to the filled one. One can choose them in the following way:

$$\begin{aligned} \Gamma_{1n} &= \bar{M}_n(1 - n_n), \\ \Gamma_{2n} &= \bar{M}_n n_n. \end{aligned} \tag{4.206}$$

Here, $\bar{M}_n$ determines the coupling strength of the n-th level to the two Markovian environments, and n_n refers to its desired occupation.

We now evaluate the corresponding auxiliary bath hybridization function $\underline{\Delta}^{Aux}$ at the impurity site. For this one should first determine the noninteracting Green's function and then use (4.199). The expression for the noninteracting Green's function of an open lattice system described by (4.161), (4.162) is evaluated in Sect. 4.9.1.1, and the expression for the Green's function matrices is given in (4.222).

For the present case it is more convenient to use (4.198) in terms of the local Green's function $\underline{g}_{nn} = \underline{g}_n$ of the n-th isolated level plus Markovian reservoir, i.e. decoupled from the impurity site. These can be determined by using (4.222) for a single site, leading to

$$\begin{aligned} g_{Rn} &= (\omega - \bar{\varepsilon}_n + i\Gamma_{+n})^{-1}, \\ g_{Kn} &= 2ig_{Rn}(\Gamma_{2n} - \Gamma_{1n})g_{Rn}^* = \frac{2i(\Gamma_{2n} - \Gamma_{1n})}{(\omega - \varepsilon_n)^2 + \Gamma_{+n}^2}. \end{aligned} \tag{4.207}$$

With (4.198), the auxiliary hybridization function on the impurity site is given by

$$\begin{aligned} \Delta_R^{Aux} &= \sum_n \bar{v}_n^2 g_{Rn}, \\ \Delta_K^{Aux} &= \sum_n \bar{v}_n^2 g_{Kn}. \end{aligned} \tag{4.208}$$

Now, the goal is to approximate the physical Δ_R, Δ_K as accurately as possible by Δ_R^{Aux} and Δ_K^{Aux}. Due to the Kramers-Kronig relation between the imaginary and the real part of retarded functions, it is sufficient to consider only the imaginary part of Δ_R, and Δ_K is itself purely imaginary. The bath spectral function, determining the DOS of the auxiliary reservoir, is given by

$$\begin{aligned} A_\Delta^{Aux}(\omega) &\equiv -\frac{1}{\pi}\Im\mathrm{m}\left\{\Delta_R^{Aux}(\omega)\right\} \\ &= \sum_n \bar{v}_n^2 \delta_{\Gamma_{+n}}(\omega - \bar{\varepsilon}_n), \end{aligned} \tag{4.209}$$

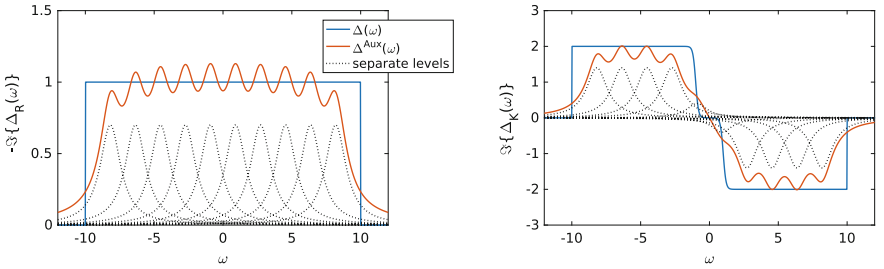

Fig. 4.12 Sketch of $\underline{\Delta}^{Aux}(\omega)$ in the buffer layer approach, with parameters chosen according to (4.211) and (4.212), and description in the text. The separate levels produce Lorentzian curves. For illustrative purposes we choose $\Gamma_{+n} = \delta_n/2$, see e.g. [95] for a detailed discussion

with the Lorentzians

$$\delta_\Gamma(\omega) \equiv \frac{1}{\pi}\frac{\Gamma}{\omega^2 + \Gamma^2}. \tag{4.210}$$

Therefore, a given physical bath spectral function $A_\Delta(\omega) = -1/\pi\,\Im\mathrm{m}\,\{\Delta_R(\omega)\}$ is approximated by a superposition of Lorentz curves, as sketched in Fig. 4.12. For equidistant levels with energies $\bar{\varepsilon}_n$ the level spacing is given by

$$\delta_n = \frac{W}{N_B}, \tag{4.211}$$

with W the bandwidth. The width of the Lorentzians (4.210) is given by Γ_{+n}, and one should choose

$$\Gamma_{+n} \approx \delta_n, \tag{4.212}$$

in order to achieve a smooth and non-peaked $A_\Delta^{Aux}(\omega)$, which reproduces features in $A_\Delta(\omega)$ properly. The hoppings $\bar{v}_n$ are then adjusted in such a way that the local density of states is correctly reproduced, and normalization requires that $\sum_n \bar{v}_n^2 = 1$. In the hypothetical $N_B \to \infty$ limit, one recovers the exact result $A_\Delta^{Aux}(\omega) \to A_\Delta(\omega)$. See [95] for a further discussion of these aspects.

Up to now we only made use of $\bar{v}_n$ and Γ_{+n}, but $\Gamma_{-n} = \Gamma_{2n} - \Gamma_{1n}$ was not determined. This remaining degree of freedom amounts to specifying the filling of each Lorentz peak $\delta_{\Gamma_{+n}}(\omega)$, and thus to adjusting the Keldysh component Δ_K^{Aux}. From (4.201) one knows that the latter is related to the spectral function via

$$\Delta_K(\omega) = -2\pi i A_\Delta(\omega) s(\omega), \tag{4.213}$$

with $s(\omega) = 1 - 2n(\omega)$ the particular equilibrium or nonequilibrium occupation. From (4.207) and (4.208) we have for the auxiliary system

$$\Delta_K^{Aux}(\omega) = 2i\pi \sum_n \bar{v}_n^2 \frac{\Gamma_{-n}}{\Gamma_{+n}} \delta_{\Gamma_+}(\omega - \bar{\varepsilon}_n), \tag{4.214}$$

which suggests to determine Γ_{-n} via

$$\frac{\Gamma_{-n}}{\Gamma_{+n}} = -s(\bar{\varepsilon}_n), \tag{4.215}$$

in order to achieve the correct $N_B \to \infty$ limit. Furthermore, when inserting (4.206) into this expression we find

$$\frac{\Gamma_{-n}}{\Gamma_{+n}} = 2n_n - 1\,, \tag{4.216}$$

and thus $s(\bar{\varepsilon}_n) = 1 - 2n_n$, as desired. For an exemplary plot of Δ_R^{Aux} and Δ_K^{Aux} with the buffer layer idea see Fig. 4.12.

4.8.2 *Finite Size Lindblad Impurity Problem*

As sketched above, in the buffer layer approach one is able to approximate the original nonequilibrium impurity model by an auxiliary one, with a finite number N_B of levels only. Most importantly, these levels are coupled to additional Markovian reservoirs in order to obtain dissipation. Once this mapping to a finite size Lindblad model has been achieved, one can solve the auxiliary manybody problem with $U \neq 0$. This is much simpler than in the original model because one only has to deal with a finite many-body Hilbert space. Appropriate methods for this, such as Lanczos ED or MPS are discussed below.

On the whole, from solving the $U \neq 0$ Lindblad model one obtains the interacting Green's function $\underline{G}^{Aux}$ on the impurity site. From the discussion at the beginning of this section it is clear that the mismatch between the auxiliary $\underline{G}^{Aux}$ and the exact $\underline{G}$ of the original model depends solely on $\|\underline{\Delta}^{Aux} - \underline{\Delta}\|$. This difference can be reduced by increasing N_B. However, a larger number of bath sites comes at the price of a drastically increased effort to address the manybody solution. For example, methods such as Lanczos ED scale exponentially in N_B. Therefore, it is highly desirable to find a mapping procedure which yields a good accuracy $\|\underline{\Delta}^{Aux} - \underline{\Delta}\| \ll \|\underline{\Delta}\|$ already for modest values of N_B. This is provided by the Auxiliary Master Equation Approach [21, 63, 78] which we present in the next section.

4.9 Auxiliary Master Equation Approach

The key idea of the auxiliary master equation approach (AMEA), introduced in [21, 63], is to make optimal use of all available parameters in the finite size Lindblad impurity model. In this way, it is possible to achieve already for small values of $N_B \approx O(10)$ a very good accuracy $\|\underline{\Delta}^{Aux} - \underline{\Delta}\| \ll \|\underline{\Delta}\|$. For this purpose we consider the *most general* quadratic Lindblad dissipator with one impurity and N_B bath levels

$$\mathcal{L}_D \rho = 2 \sum_{n,m=1}^{N_B} \left(\Gamma_{1mn} \left(d_n \rho d_m^\dagger - \frac{1}{2} \{ d_m^\dagger d_n, \rho \} \right) + \Gamma_{2mn} \left(d_m^\dagger \rho d_n - \frac{1}{2} \{ d_n d_m^\dagger, \rho \} \right) \right). \tag{4.217}$$

Note here the important aspect that the coupling matrices Γ_{1nm} and Γ_{2nm} to the Markovian environments are *non diagonal*, in contrast to (4.205), i.e. every possible coupling is included. The unitary part of the Lindblad equation can be chosen to be sparse, even in the most general case, since one always has the freedom to perform unitary transformations among bath sites only, since it does not affect $\underline{\Delta}^{Aux}$ on the impurity site. Therefore, the N_B bath sites can be assumed to be either in a chain or star geometry. The former case is schematically depicted in Fig. 4.13. In the latter case, in addition to Γ_{1nm} and Γ_{2nm}, we have the Hamiltonian parameters $\bar{\varepsilon}_n$ and $\bar{v}_n$. In AMEA all these parameters are optimized in a fit procedure by minimizing the difference between $\underline{\Delta}^{Aux}$ and $\underline{\Delta}$. We again stress that *the better* $\underline{\Delta}^{Aux}$ *approaches* $\underline{\Delta}$, *the better the accuracy of the impurity solver is.* In order to carry out the fit, we define the cost function

$$\chi(\bar{\varepsilon}, \bar{v}, \Gamma) = \int d\omega \| \Im \mathrm{m} \left\{ \underline{\Delta}^{Aux}(\omega) - \underline{\Delta}(\omega) \right\} \|^2 , \tag{4.218}$$

and minimize it with respect to $\{\Gamma_{1nm}, \Gamma_{2nm}, \bar{\varepsilon}_n, \bar{v}_n\}$. On the whole, this amounts to solving a multi-dimensional optimization problem with $O(N_B^2)$ parameters. Even though this procedure is more involved than the simple choice of $\{\Gamma_{1nn}, \Gamma_{2nn}, \bar{\varepsilon}_n, \bar{v}_n\}$

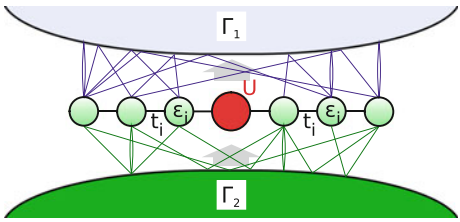

Fig. 4.13 Auxiliary master equation approach: The reservoirs are represented by a finite number of levels coupled to two Markovian environments. In contrast to the buffer layer approach, Fig. 4.11, all possible couplings are allowed, so that the coupling matrices Γ_{1nm} and Γ_{2nm} are *non diagonal*. Again, the system is governed by a Lindblad equation (4.217)

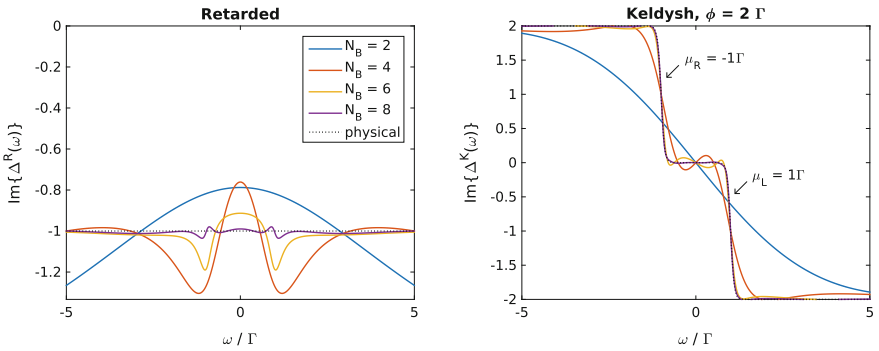

Fig. 4.14 Results for $\underline{\Delta}^{Aux}(\omega)$ in the auxiliary master equation approach, for a physical $\underline{\Delta}(\omega)$ similar to the one in Fig. 4.12. Already for real, dense Γ_{1nm} and Γ_{2nm} matrices, a rapid convergence with increasing N_B is observed, see also [63, 71, 78]. The bias voltage between left and right lead is denoted by ϕ, and Γ refers to the hybridization strength of the leads

in the buffer layer idea discussed above, the key aspect is that one achieves here an exponential convergence of $\underline{\Delta}^{Aux}$ towards $\underline{\Delta}$ with increasing N_B, see also [71]. Exemplary results for this fitting procedure are depicted in Fig. 4.14. More details can be found in [71].

Once the parameters of the auxiliary system are fitted, the interacting Lindblad equation must be solved. Up to now, we employed for this two different strategies based on ED and MPS, respectively, see [63] and [78] for details. The former allows us to consider all possible couplings so that modest values of $N_B = 6$ are sufficient for an accurate representation of the reservoirs, see Fig. 4.14. In the latter case we restricted the fit to sparse Γ_{1nm} and Γ_{2nm} matrices, in order to be able to apply efficient MPS techniques. The restriction results in not as optimal fits as with dense Γ_{1nm} and Γ_{2nm}, but, due to MPS much larger system sizes of $N_B = 15 - 20$ are possible, which outweighs and yields a significantly improved accuracy compared to the ED solver.

In the figures below, we present exemplary results for the ED and the MPS approach. In Figs. 4.15 and 4.16 ED results for a semi-circular lead DOS are shown. With the MPS approach we focused on the low-bias regime and considered a wide band model for the leads, as plotted in Figs. 4.12 and 4.14. Very accurate spectral functions could be obtained and it was possible for us to resolve the splitting of the Kondo peak with increasing bias voltage $\phi = \mu_L - \mu_R$ in detail, see Figs. 4.17, 4.18 and 4.19.

4.9.1 Evaluation of Steady State Green's Functions

We now focus on the computation of the steady state Green's functions in the auxiliary Lindblad system. At first we consider the noninteracting case, for which compact expressions are derived. These are crucial for AMEA in order to efficiently compute

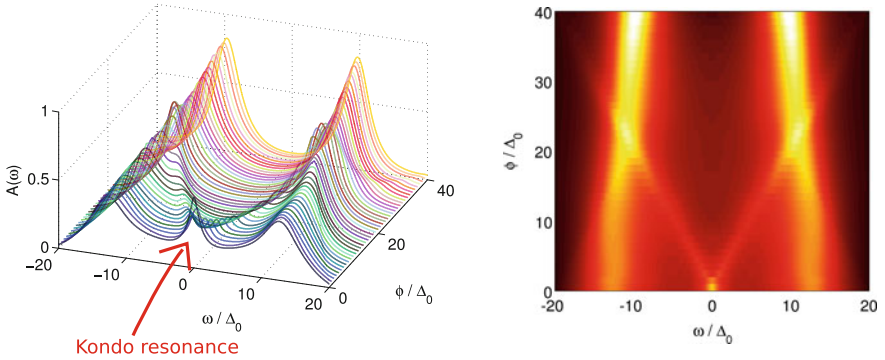

Fig. 4.15 ED results for the evolution of the impurity spectral function $A(\omega)$ with increasing bias voltage ϕ. In the equilibrium limit $\phi = 0$, a distinct Kondo peak and two Hubbard bands are clearly visible. The former splits upon increasing ϕ into two weak excitations, which are located at the positions of the chemical potentials $\mu_{\pm} = \pm\phi/2$. Results taken from [63], for an interaction strength $U = 20\,\Delta_0$, with Δ_0 half the hybridization strength of the leads

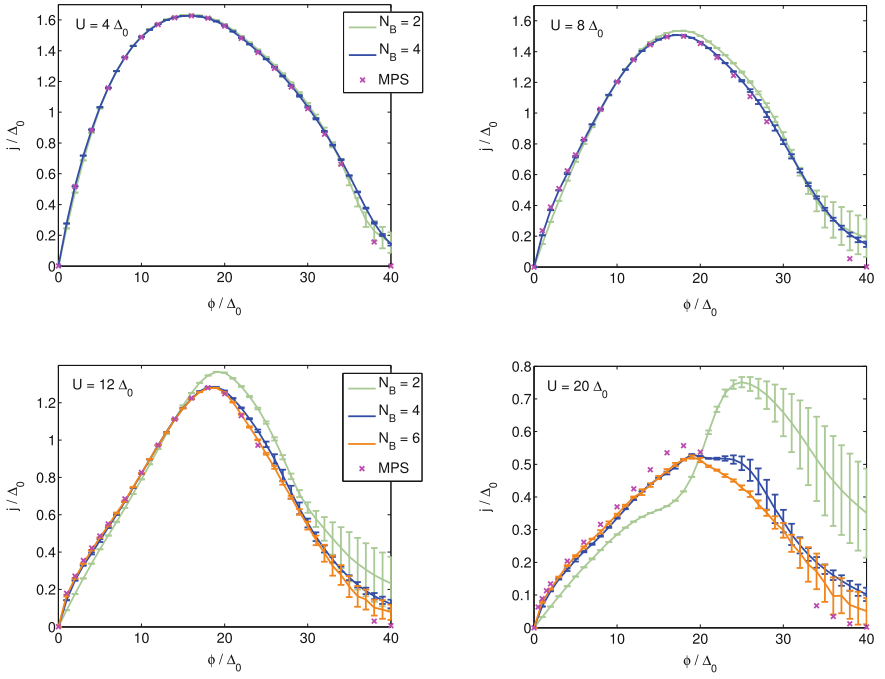

Fig. 4.16 ED results for the current-voltage characteristics of the nonequilibrium SIAM with semicircular lead DOS. At the lead bandwidth $\phi = 40\,\Delta_0$, the current is strongly suppressed and must vanish for $U = 0$. MPS refers to quasi exact reference data [61]. Results taken from [63]

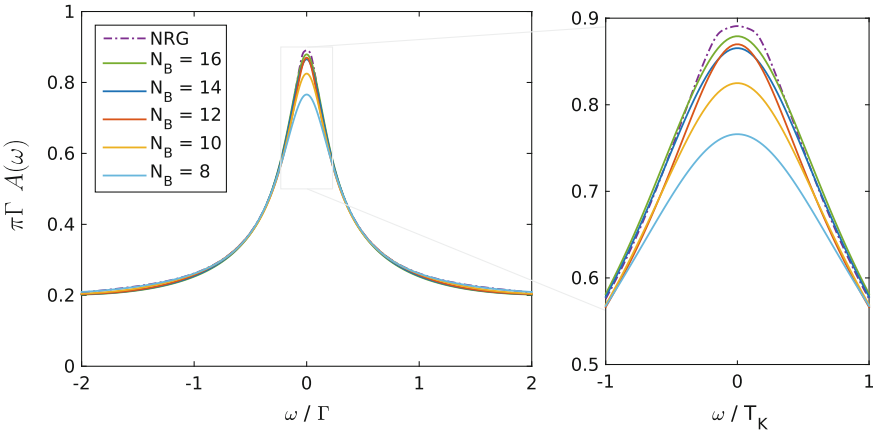

Fig. 4.17 MPS results for the equilibrium, i.e. $\phi = 0$, spectral function with increasing number of bath sites. A comparison to a quasi exact NRG reference calculation reveals a remarkably close agreement. Results for a temperature $T = 0.05\Gamma$ well below the Kondo scale $T_K \approx 0.2\Gamma$, taken from [78] (For $T/T_K \to 0$ the exact spectral function fullfills the so-called Friedel sum rule $A(\omega) = \pi\Gamma$.)

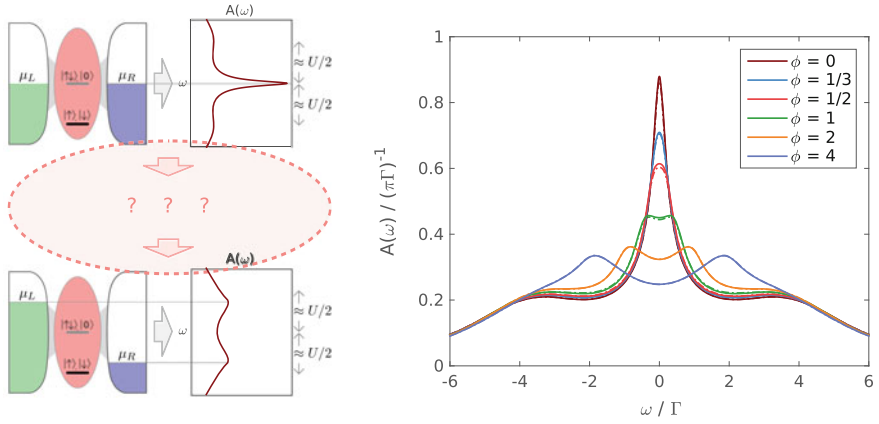

Fig. 4.18 Sketch of the nonequilibrium impurity problem on the left. In the low energy limit $\phi \ll T_K$, as well as in the high energy limit $\phi \gg T_K$, the detailed physics is known. On the right we present MPS results for the nonequilibrium spectral function in the challenging intermediate regime $T < T_K$ and $\phi \sim T_K$, displaying a clear splitting of the Kondo peak for $\phi > \Gamma/2$. Figure on the right taken from [78]

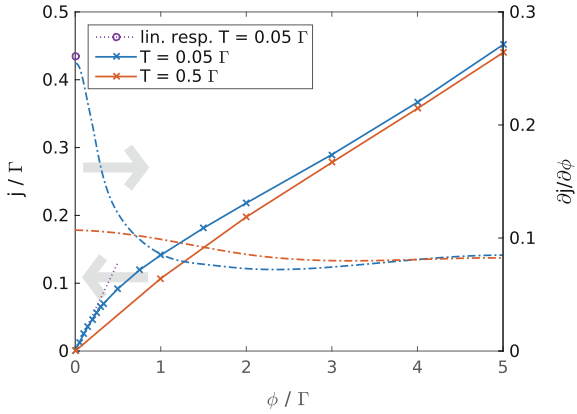

Fig. 4.19 MPS results for the current-voltage characteristics together with the differential conductance $\partial j/\partial\phi$. At low temperatures and close to $\phi \approx 0$, a clear enhancement of the conductivity due to the Kondo effect is found. Figure taken from [78]

$\underline{\Delta}^{Aux}(\omega)$, and thus, for fitting $\underline{\Delta}^{Aux}(\omega)$ to $\underline{\Delta}(\omega)$ by minimizing (4.218). After that we focus on the manybody problem and the computation of the interacting Green's function $\underline{G}^{Aux}$.

4.9.1.1 Noninteracting Case

We start from (4.153), (4.154) and (4.155), i.e. the Lindblad equation in superfermion representation. This equation of "Schrödinger type" can be rewritten in the following form

$$i\mathcal{L} = \underline{\underline{C}}^{\dagger}\,\underline{\underline{H}}\,\underline{\underline{C}} + \text{const.}, \tag{4.219}$$

where

$$\underline{\underline{C}} = \begin{pmatrix} c_1 \\ \vdots \\ c_N \\ \tilde{c}_1^{\dagger} \\ \vdots \\ \tilde{c}_N^{\dagger} \end{pmatrix} \tag{4.220}$$

summarizes the fermionic operators c_i ($\tilde{c}_i^{\dagger}$) for original (tilde) sites, and

$$\begin{aligned} \underline{\underline{H}} &= \begin{pmatrix} E_+ & B \\ \bar{B} & E_- \end{pmatrix}, \\ E_{\pm} &= E \pm i(\Gamma_2 - \Gamma_1), \\ B &= 2\Gamma_2, \\ \bar{B} &= -2\Gamma_1. \end{aligned} \tag{4.221}$$

The matrix E accounts hereby for all single-particle terms in the original Hamiltonian, i.e. all hoppings and onsite energies, and the dense matrices $\Gamma_{1/2}$ contain all the couplings to the Markovian environments, see (4.217).

The detailed derivation of the Green's functions for the generic case of a lattice model is rather lengthy and can be found for instance in [63, 95]. On the other hand, the final expression is quite compact, so we start by displaying it here in matrix form in the i, j indices

$$\begin{aligned} G_R(\omega) &= (\omega - E + i\Gamma_+)^{-1}, \\ G_K(\omega) &= 2i\, G_R(\omega)\Gamma_- G_A(\omega), \end{aligned} \tag{4.222}$$

with the abbreviations $\Gamma_\pm = \Gamma_2 \pm \Gamma_1$. These analytic expressions involve only matrix multiplications of size $N = N_B + 1$ and are thus numerically cheap to evaluate. We now prove (4.222).

Proof for the Retarded Component

The retarded Green's function is given by

$$\begin{aligned} G_R(t)_{\alpha\beta} &= -i\theta(t)\langle\{c_\alpha(t), c_\beta^\dagger\}\rangle \\ &= \theta(t)(p_{\alpha\beta}(t) + g_{\alpha\beta}(t)), \end{aligned} \tag{4.223}$$

with the first part

$$\begin{aligned} p_{\alpha\beta}(t) &= -i\mathrm{Tr} c_\alpha (c_\beta^\dagger \rho)_t = -i\langle I|c_\alpha (c_\beta^\dagger \rho)_t|I\rangle \\ &= -i\langle I|c_\alpha e^{\mathcal{L}t} c_\beta^\dagger|\rho\rangle \equiv -i\langle I|c_\alpha|c_\beta^\dagger(t)\rangle, \end{aligned} \tag{4.224}$$

where ρ is in the steady state, and the usual restriction $t > 0$ of the Lindblad formalism applies. When making use of the property $\langle I|\mathcal{L} = 0$ one can write the time derivative in terms of an equation of motion

$$\frac{d}{dt} p_{\alpha\beta}(t) = -i\langle I|[c_\alpha, \mathcal{L}]|c_\beta^\dagger(t)\rangle. \tag{4.225}$$

With the Lindblad operator in the form of (4.219) one finds for the commutator

$$\begin{aligned} [c_\alpha, i\mathcal{L}] &= \sum_{\tilde{\gamma}=1}^{2N} \underline{\underline{H}}_{\alpha\tilde{\gamma}}\, \underline{\underline{C}}_{\tilde{\gamma}} \\ &= \sum_{\gamma=1}^{N} \left(E_{+\alpha\gamma}\, c_\gamma + B_{\alpha\gamma}\, \tilde{c}_\gamma^\dagger\right), \end{aligned} \tag{4.226}$$

where we made use of the definition (4.220) in the second line. Multiplied with the left vacuum this results in terms of the form

$$\langle I|[c_\alpha, i\mathcal{L}] \to \sum_\gamma (E_+ - iB)_{\alpha\gamma} \langle I|c_\gamma = \sum_\gamma (E - i\Gamma_+)_{\alpha\gamma} \langle I|c_\gamma, \tag{4.227}$$

due to the tilde conjugation rule $\langle I|\tilde{c}^\dagger = -i\langle I|c$. In matrix notation one thus arrives at

$$\frac{d}{dt}p = -i(E - i\Gamma_+)p. \tag{4.228}$$

Now, we proceed analogously with the second part

$$g_{\alpha\beta}(t) = -i\mathrm{Tr}(c_\beta^\dagger c_\alpha(t)\rho) = -i\mathrm{Tr}c_\alpha(\rho c_\beta^\dagger)_t. \tag{4.229}$$

In terms of Lindblad time evolution and with the help of the tilde conjugation rules we find that

$$\begin{aligned} g_{\alpha\beta}(t) &= -i\langle I|c_\alpha e^{\mathcal{L}t}\rho c_\beta^\dagger|I\rangle = -i\langle I|c_\alpha e^{\mathcal{L}t}(-i\tilde{c}_\beta)|\rho\rangle \\ &= -\langle I|c_\alpha e^{\mathcal{L}t}\tilde{c}_\beta|\rho\rangle = -\langle I|c_\alpha|\tilde{c}_\beta(t)\rangle. \end{aligned} \tag{4.230}$$

In the same manner as before, by writing down the equations of motion one arrives at

$$\frac{d}{dt}g = -i(E - i\Gamma_+)g. \tag{4.231}$$

Finally, from inserting the results (4.228) and (4.231) into the time derivative of (4.223), one finds the following equation of motion for the retarded Green's function

$$i\frac{d}{dt}G_R(t) = I\delta(t) + (E - i\Gamma_+)G_R(t). \tag{4.232}$$

Fourier transforming of the lhs and rhs of the equation yields $\int i\frac{d}{dt}G_R(t)e^{i\omega t}dt = \omega G_R(\omega)$ and $I + (E - i\Gamma_+)G_R(\omega)$. Overall this results in the first equation in (4.222). The effective broadening Γ_+ corresponds in real time to a damping: $G_R(t) = \int_{-\infty}^{+\infty} G_R(\omega)e^{-i\omega t}\frac{d\omega}{2\pi} \sim e^{-\Gamma_+ t}$ for $t > 0$.

In analogous manner one obtains for the advanced Green's function the usual relation

$$\begin{aligned} G_A(\omega) &= G_R(\omega)^\dagger \\ &= (\omega - E - i\Gamma_+)^{-1}. \end{aligned} \tag{4.233}$$

Proof for the Keldysh component

For the Keldysh component we follow closely the one presented in [95]. Analogous to (4.223), G_K is given by

$$\begin{aligned} G_K(t) &= -i\langle [c(t), c^\dagger] \rangle \\ &= p(t) - g(t), \end{aligned} \tag{4.234}$$

when written in matrix form. Using the expressions for $p(t)$ and $g(t)$ derived above, one has for $t > 0$

$$i\frac{d}{dt}G_K(t) = (E - i\Gamma_+)G_K(t), \tag{4.235}$$

with the solution

$$G_K(t > 0) = e^{-i(E-i\Gamma_+)t} \underbrace{G_{K0}}_{G_K(t=0)} . \tag{4.236}$$

For $t < 0$ one can use the following property

$$G_K(t) = -G_K(-t)^\dagger, \tag{4.237}$$

which is easily verified by inserting the definition of G_K, (4.234). For negative times one thus has

$$G_K(t < 0) = G_{K0} e^{-i(E+i\Gamma_+)t}, \tag{4.238}$$

since $G_{K0}^\dagger = -G_{K0}$. When splitting the time integration in the Fourier transform, one finds from (4.236) and (4.238)[22]

$$\begin{aligned} G_K(\omega) &= \int_{-\infty}^{+\infty} dt e^{i\omega t} G_K(t) \\ &= i(\omega - E + i\Gamma_+)^{-1} G_{K0} - i G_{K0}(\omega - E - i\Gamma_+)^{-1} \\ &= i(G_R(\omega) G_{K0} - G_{K0} G_A(\omega)). \end{aligned} \tag{4.239}$$

From the Langreth rules, (4.190), one has for the inverse

$$[\underline{G}(\omega)^{-1}]_K = -i(G_{K0} G_A(\omega)^{-1} - G_R(\omega)^{-1} G_{K0}), \tag{4.240}$$

and G_{K0} is given by the equal time expectation value

$$\begin{aligned} G_{K0} &= -i(2m - I), \\ m_{\alpha\beta}(t) &= \langle c_\alpha c_\beta^\dagger \rangle_t. \end{aligned} \tag{4.241}$$

From the corresponding equation of motion we now determine the steady state expression for $m_{\alpha\beta}(t)$:

[22] Cf. Generalized Kadanoff-Baym ansatz (GKBA) [99].

$$0 = \frac{dm_{\alpha\beta}}{dt} = \frac{d}{dt}\langle c_\alpha c_\beta^\dagger\rangle = \langle I|[c_\alpha c_\beta^\dagger, \mathcal{L}]|\rho(t)\rangle = \langle I|(c_\alpha[c_\beta^\dagger, \mathcal{L}] + [c_\alpha, \mathcal{L}]c_\beta^\dagger)|\rho\rangle. \tag{4.242}$$

For the sake of clarity we omit matrix indices. Using (4.219) for the Lindblad operator we obtain

$$\begin{aligned}\frac{dm}{dt} &= -i\langle I|c(-\underline{\underline{C}}^\dagger \underline{\underline{H}})|\rho\rangle - i\langle I|(\underline{\underline{H}}\,\underline{\underline{C}})c^\dagger|\rho\rangle \\ &= i\langle I|c(c^\dagger E_+ + \tilde{c}\bar{B})|\rho\rangle - i\langle I|(E_+ c + B\tilde{c}^\dagger)c^\dagger|\rho\rangle \\ &= imE_+ - \underbrace{\langle I|c^\dagger c|\rho\rangle}_{1-m}\bar{B} - iE_+ m - Bm,\end{aligned} \tag{4.243}$$

where in the last line we have made use of the tilde conjugation rules. On the whole, the steady-state single particle density matrix $1 - m$ is obtained from solving

$$(m-1)\bar{B} - Bm - i[E_+, m] = 0. \tag{4.244}$$

With the definitions from (4.221) and (4.241) this amounts to

$$2\Gamma_- = (E - i\Gamma_+)G_{K0} - G_{K0}(E + i\Gamma_+). \tag{4.245}$$

The rhs is just what is obtained from (4.240), when inserting the expressions for $G_{R/A}(\omega)$:

$$\begin{aligned}[\underline{G}(\omega)^{-1}]_K &= -i(G_{K0}G_A(\omega)^{-1} - G_R(\omega)^{-1}G_{K0}) \\ &= -i(G_{K0}(\omega - E - i\Gamma_+) - (\omega - E + i\Gamma_+)G_{K0}) \\ &= 2i\Gamma_-.\end{aligned} \tag{4.246}$$

4.9.1.2 Interacting Case

To solve the interacting problem we set up the full manybody basis in the superfermion representation, which corresponds to the manybody Hilbert space for (density) operators of the $N = N_B + 1$ sites system. The Hilbert space size is exponentially large, $N_{\mathcal{H}} = 16^N$, when taking both spin directions and no particle conservation into account. In the following we assume that the Lindblad operator and the corresponding manybody states are expressed in this basis, so that the time evolution equation

$$|\rho(t)\rangle = e^{\hat{\mathcal{L}}t}|\rho(0)\rangle, \tag{4.247}$$

corresponds to a linear algebra problem of size $N_{\mathcal{H}}$. As before, $i\hat{\mathcal{L}}$ plays the role of a non-Hermitian Hamiltonian.

We assume that $\hat{\mathcal{L}}$ can be diagonalized, a property which is not trivial for a non-Hermitian matrix but can be argued from a physical point of view. The left- and right-sided eigenvectors

$$\begin{aligned} \hat{\mathcal{L}}|\alpha R\rangle &= \mathcal{L}_\alpha |\alpha R\rangle, \\ \langle \alpha L|\hat{\mathcal{L}} &= \mathcal{L}_\alpha \langle \alpha L|\,, \end{aligned} \tag{4.248}$$

with eigenvalues $\mathcal{L}_\alpha$ can be chosen in such a way that they are bi-orthogonal to each other

$$\langle \alpha L|\beta R\rangle = \delta_{\alpha\beta}, \tag{4.249}$$

and form a complete set,

$$\hat{I} = \sum_\alpha |\alpha R\rangle\langle \alpha L|. \tag{4.250}$$

Due to this we can expand any state $|\rho(t)\rangle$ in this basis and one can rewrite (4.247) as

$$\begin{aligned} |\rho(t)\rangle &= \sum_\alpha P_\alpha(t)|\alpha R\rangle, \\ P_\alpha(t) &= e^{\mathcal{L}_\alpha t} P_\alpha(0). \end{aligned} \tag{4.251}$$

For a stable solution one must have that $\Re\{\mathcal{L}_\alpha\} \leq 0$, which is ensured by the form of the Lindblad equation. Furthermore, at least one eigenvalue must be zero due to the property $\langle I|\hat{\mathcal{L}} = 0$ of the left vacuum, (4.157). We assume here that exactly one eigenvalue, say $\mathcal{L}_{\alpha=0}$, is zero with the following two corresponding left and right eigenstates

$$\begin{aligned} \langle I| &= \langle \alpha = 0, L|, \\ |\rho_\infty\rangle &= |\alpha = 0, R\rangle, \end{aligned} \tag{4.252}$$

where $|\rho_\infty\rangle$ is the steady state. From (4.249) it follows that

$$\langle I|\rho_\infty\rangle = 1, \tag{4.253}$$

which is just the trace normalization of the density matrix. The assumption that only one eigenvalue is zero, and, more generally, that only one has a vanishing real part, is expected to be fullfilled for systems in which each level which is connected to a Lindblad coupling. In this case, any initial state is expected to dissipate so that a unique steady state is fullfilled.

In order to reduce the relevant Hilbert space size $N_{\mathcal{H}}$ it is expedient to make use of conserved quantities. In many interesting cases, the number of particles per spin component is conserved. Within the superfermion representation this translates into the conservation of the operator[23]

$$\begin{aligned}\Delta_\sigma &= N_\sigma - \tilde{N}_\sigma \\ &= \sum_i \left(c_{i\sigma}^\dagger c_{i\sigma} - \tilde{c}_{i\sigma}^\dagger \tilde{c}_{i\sigma} \right)\end{aligned} \tag{4.254}$$

The left vacuum $\langle I|$ and, consequently also the steady state $|\rho_\infty\rangle$ are situated in the sector $\Delta_\sigma = 0$, as can be easily checked. The excited states used to evaluate Green's function belong to sectors with one of the $\Delta_\sigma \neq 0$. For example, $|c_\uparrow^\dagger(t)\rangle = e^{\mathcal{L}t} c_\uparrow^\dagger |\rho_\infty\rangle$ has $\Delta_\uparrow = 1$ and $\Delta_\downarrow = 0$. A general non-stationary state $|\rho(t)\rangle$ which is not an eigenstate of $\mathcal{L}$, however, does not necessarily have a well-defined particle sector Δ_σ. From (4.251) it follows that in this case all components with $\Delta_\sigma \neq 0$ are exponentially damped and only the steady state component $|\alpha = 0, R\rangle$ in the sector $\Delta_\sigma = 0$ survives in the long-time limit. Thus, for the purpose of finding the steady state $|\rho_\infty\rangle$, a convenient choice for the initial state is for instance $|\rho(t=0)\rangle = |I\rangle$.[24]

Steady State Correlation Functions

Here we show that correlation functions in the steady state can be expressed in the form of a Lehmann representation, analogous to the equilibrium case (cf. [63, 100]). The steady state Green's function in the time domain, $iG_{BA}(t) \equiv \langle B(t)A\rangle$, reads in terms of the superfermion representation

$$\begin{aligned}iG_{BA}(t,+) &\equiv \theta(t)\langle I|B|A(t)\rangle \\ &= \theta(t)\langle I|Be^{\mathcal{L}t}A|\rho_\infty\rangle,\end{aligned} \tag{4.255}$$

where $+$ indicates that the time argument is ≥ 0 and one can use the "normal" quantum regression theorem, see Sect. 4.6. When inserting the identity operator in terms of the eigenstates of $\mathcal{L}$, (4.250), one obtains

$$\begin{aligned}iG_{BA}(t,+) &= \theta(t)\langle 0L|BIe^{\mathcal{L}t}IA|0R\rangle \\ &= \theta(t)\sum_\alpha \langle 0L|B|\alpha R\rangle\langle \alpha L|A|0R\rangle e^{\mathcal{L}_\alpha t},\end{aligned} \tag{4.256}$$

[23] Also the analogue to the usual SU(2) spin symmetry can be implemented, although it is more involved.

[24] Note that a more standard form for the conserved quantities is obtained when performing a particle-hole transformation in the tilde space $\tilde{c}_\sigma \to \tilde{h}_\sigma^\dagger$, since then $\Delta_\sigma \to N_\sigma + \tilde{N}_\sigma - N$.

and subsequent Fourier transformation yields

$$\begin{aligned} G_{BA}(\omega,+) &= \int_{-\infty}^{\infty} G_{BA}(t,+)e^{i\omega t}dt \\ &= \sum_{\alpha} \langle 0L|B|\alpha R\rangle\langle \alpha L|A|0R\rangle \frac{1}{\omega - i\mathcal{L}_{\alpha}}. \end{aligned} \tag{4.257}$$

In particular we are interested in the retarded and Keldysh Green's functions. The retarded Green's function in the time domain is given by

$$\begin{aligned} G_{RBA}(t) &= -i\theta(t)\langle\{B(t),A\}\rangle \\ &= -i\theta(t)\langle B(t)A + A(-t)B\rangle \\ &= G_{BA}(t,+) + G_{AB}(-t,-), \end{aligned} \tag{4.258}$$

where the QRT cannot be applied directly to the second term. But, as before, from the complex conjugate one finds

$$\begin{aligned} iG_{AB}(-t,-) &\equiv \theta(t)\langle AB(t)\rangle \\ &= \theta(t)\langle B^{\dagger}(t)A^{\dagger}\rangle^{*} \\ &= \theta(t)\langle I|B^{\dagger}|A^{\dagger}(t)\rangle^{*} \\ &= \theta(t)\left(\sum_{\alpha}\langle 0L|B^{\dagger}|\alpha R\rangle\langle \alpha L|A^{\dagger}|0R\rangle e^{\mathcal{L}_{\alpha}t}\right)^{*}, \end{aligned} \tag{4.259}$$

and the Fourier transform is given by

$$\begin{aligned} G_{AB}(\omega,-) &= \int_{-\infty}^{\infty} G_{AB}(-t,-)e^{i\omega t}dt \\ &= \sum_{\alpha}\left(\langle 0L|B^{\dagger}|\alpha R\rangle\langle \alpha L|A^{\dagger}|0R\rangle\right)^{*}\frac{1}{\omega - i\mathcal{L}_{\alpha}^{*}}. \end{aligned} \tag{4.260}$$

On the whole, $G_{RBA}(\omega)$ is obtained by the Fourier transform of (4.258), so by the sum of (4.257) and (4.260). In particular, one can see that the poles are located at $\omega = i\mathcal{L}_{\alpha}$ and $\omega = i\mathcal{L}_{\alpha}^{*}$, so in the lower complex half plane since $\Re\{\mathcal{L}_{\alpha}\} \leq 0$ for all eigenstates. This ensures the causality of the retarded Green's functions. Due to these poles away from the real axis, the spectrum is not given by a sum of delta peaks, as for a finite size system, but by a continuous function.

The Lehmann representation of $G_{KAB}(\omega)$ is obtained in a similar way, leading to

$$\begin{aligned} G_{KAB}(\omega) &= -i\mathcal{F}\{\langle [B(t), A]\rangle\} \\ &= \sum_{\alpha} \langle 0L|B|\alpha R\rangle \langle \alpha L|A|0R\rangle \frac{1}{\omega - i\mathcal{L}_{\alpha}} \\ &+ \sum_{\alpha} \langle 0L|A|\alpha R\rangle \langle \alpha L|B|0R\rangle \frac{1}{\omega + i\mathcal{L}_{\alpha}} - \text{h.c.} \end{aligned} \tag{4.261}$$

with $\mathcal{F}\{\}$ denoting the Fourier transformation and h.c. stands for the Hermitian conjugate of the two sums.

In practice, the Green's functions described above can be determined either directly by full diagonalization of the Lindblad operator, see (4.248), or with Krylov space methods. A full diagonalization is only feasible for rather small matrices of size $N_{\mathcal{H}} \lesssim 5000$, due to memory constraints and since the numerical effort scales with the third power of the matrix size. Krylov space methods, on the other hand, allow one to consider much larger values of $N_{\mathcal{H}} \approx 10^7 - 10^9$, because only matrix-vector products are needed. Instead of computing all eigenvectors of the Lindblad operator, only the relevant subset, the so-called Krylov subspace is targeted in an iterative fashion. For the case of Green's functions, for instance, $\langle l|1/(\omega - \alpha\mathcal{L})|r\rangle$ is computed by forming a bi-orthogonal set of vectors spanned by $\langle l|\mathcal{L}^n$ and $\mathcal{L}^n|r\rangle$ with $n = 0, 1, 2, \ldots$. For more details on the common Lanczos algorithm for Hermitian problems, as well as the bi- or two-sided Lanczos and the Arnoldi algorithm for non-Hermitian matrices, which must be used in the present problem, we refer to [101–103].

Acknowledgements We gratefully acknowledge fruitful discussions with Michael Knap, Delia Fugger, Max Sorantin, Irakli Titvinidze, Frauke Schwarz, Jan von Delft, Sebastian Diehl, Wolfgang von der Linden, Hans Gerd Evertz, and Martin Nuss. Special thanks to Manuel Alamo, Fabio Covito, Daniel May, Matthias Peschke, and Christian Schäfer for help with the preparation of the manuscript. Thanks also to Roberta Citro and Ferdinando Mancini for the organization of this school. This work was partially supported by the Austrian Science Fund (FWF) within Projects P26508, and F41 (SFB ViCoM), as well as NaWi Graz. The calculations were partly performed on the D-Cluster Graz and on the VSC-3 cluster Vienna.

References

1. H. Haug, A.P. Jauho, *Quantum Kinetics in Transport and Optics of Semiconductors* (Springer, Heidelberg, 1998). http://www.springer.com/us/book/9783540735618
2. J. Rammer, H. Smith, Rev. Mod. Phys. **58**, 323 (1986). https://doi.org/10.1103/RevModPhys.58.323
3. P.W. Anderson, Phys. Rev. **124**, 41 (1961). https://doi.org/10.1103/PhysRev.124.41
4. J. Kondo, Progress Theor. Phys. **32**(1), 37 (1964). https://doi.org/10.1143/PTP.32.37. http://ptp.ipap.jp/link?PTP/32/37/
5. J.R. Schrieffer, P.A. Wolff, Phys. Rev. **149**, 491 (1966). https://doi.org/10.1103/PhysRev.149.491

6. A.C. Hewson, *The Kondo Problem to Heavy Fermions* (Cambridge University Press, Cambridge, 1993). https://doi.org/10.1017/CBO9780511470752 (Cambridge Books Online)
7. R. Bulla, T.A. Costi, T. Pruschke, Rev. Mod. Phys. **80**(2), 395 (2008). https://doi.org/10.1103/RevModPhys.80.395
8. M. Caffarel, W. Krauth, Phys. Rev. Lett. **72**(10), 1545 (1994). https://doi.org/10.1103/PhysRevLett.72.1545
9. A. Georges, G. Kotliar, W. Krauth, M.J. Rozenberg, Rev. Mod. Phys. **68**, 13 (1996). https://doi.org/10.1103/RevModPhys.68.13
10. H. Aoki, N. Tsuji, M. Eckstein, M. Kollar, T. Oka, P. Werner, Rev. Mod. Phys. **86**, 779 (2014). https://doi.org/10.1103/RevModPhys.86.779
11. P. Schmidt, H. Monien, Nonequilibrium dynamical mean-field theory of a strongly correlated system (2002). http://arxiv.org/abs/cond-mat/0202046
12. J.K. Freericks, V.M. Turkowski, V. Zlatić, Phys. Rev. Lett. **97**(26), 266408 (2006). https://doi.org/10.1103/PhysRevLett.97.266408
13. J.K. Freericks, Phys. Rev. B **77**(7), 075109 (2008). https://doi.org/10.1103/PhysRevB.77.075109
14. A.V. Joura, J.K. Freericks, T. Pruschke, Phys. Rev. Lett. **101**(19), 196401 (2008). https://doi.org/10.1103/PhysRevLett.101.196401. http://link.aps.org/abstract/PRL/v101/e196401
15. M. Moeckel, S. Kehrein, Phys. Rev. Lett. **100**, 175702 (2008). https://doi.org/10.1103/PhysRevLett.100.175702
16. M. Eckstein, M. Kollar, P. Werner, Phys. Rev. Lett. **103**, 056403 (2009). https://doi.org/10.1103/PhysRevLett.103.056403
17. S. Okamoto, Phys. Rev. B **76**, 035105 (2007). https://doi.org/10.1103/PhysRevB.76.035105
18. S. Okamoto, Phys. Rev. Lett. **101**, 116807 (2008). https://doi.org/10.1103/PhysRevLett.101.116807
19. A. Amaricci, C. Weber, M. Capone, G. Kotliar, Phys. Rev. B **86**, 085110 (2012). https://doi.org/10.1103/PhysRevB.86.085110
20. E. Munoz, C.J. Bolech, S. Kirchner, Phys. Rev. Lett. **110**, 016601 (2013)
21. E. Arrigoni, M. Knap, W. von der Linden, Phys. Rev. Lett. **110**, 086403 (2013). https://doi.org/10.1103/PhysRevLett.110.086403
22. I. Titvinidze, A. Dorda, W. von der Linden, E. Arrigoni, Phys. Rev. B **92**, 245125 (2015). https://doi.org/10.1103/PhysRevB.92.245125
23. A. Dorda, I. Titvinidze, E. Arrigoni, J. Phys.: Conf. Ser. **696**(1), 012003 (2016). https://doi.org/10.1088/1742-6596/696/1/012003
24. G. Mazza, A. Amaricci, M. Capone, M. Fabrizio, Phys. Rev. Lett. **117**, 176401 (2016). https://doi.org/10.1103/PhysRevLett.117.176401
25. M. Rigol, Phys. Rev. A **80**, 053607 (2009). https://doi.org/10.1103/PhysRevA.80.053607
26. J.H. Shirley, Phys. Rev. **138**, B979 (1965). https://doi.org/10.1103/PhysRev.138.B979
27. R. Citro, N. Andrei, Q. Niu, Phys. Rev. B **68**, 165312 (2003). https://doi.org/10.1103/PhysRevB.68.165312
28. A. Russomanno, S. Pugnetti, V. Brosco, R. Fazio, Phys. Rev. B **83**, 214508 (2011). https://doi.org/10.1103/PhysRevB.83.214508
29. A.K. Eissing, V. Meden, D.M. Kennes, Phys. Rev. Lett. **116**, 026801 (2016). https://doi.org/10.1103/PhysRevLett.116.026801
30. N.S. Wingreen, K.W. Jacobsen, J.W. Wilkins, Phys. Rev. Lett. **61**(12), 1396 (1988). https://doi.org/10.1103/PhysRevLett.61.1396
31. J.X. Zhu, A.V. Balatsky, Phys. Rev. B **67**, 165326 (2003). https://doi.org/10.1103/PhysRevB.67.165326
32. T. Brandes, Phys. Rep. **408**(5–6), 315 (2005). https://doi.org/10.1016/j.physrep.2004.12.002. http://www.sciencedirect.com/science/article/B6TVP-4FCSDMG-2/2/f74e72e3efc0ee8b22029719949f565f
33. T. Yamamoto, K. Watanabe, Phys. Rev. Lett. **96**, 255503 (2006). https://doi.org/10.1103/PhysRevLett.96.255503

34. J. Loos, T. Koch, A. Alvermann, A.R. Bishop, H. Fehske, J. Phys. Condens. Matter **21**(39), 395601 (2009). http://stacks.iop.org/0953-8984/21/i=39/a=395601
35. M. Galperin, A. Nitzan, M.A. Ratner, Phys. Rev. B **75**, 155312 (2007). https://doi.org/10.1103/PhysRevB.75.155312
36. T.A. Costi, A.C. Hewson, V. Zlatic, J. Phys. Condens. Matter **6**(13), 2519 (1994). http://stacks.iop.org/0953-8984/6/i=13/a=013
37. K.G. Wilson, Rev. Mod. Phys. **47**, 773 (1975)
38. E. Gull, A.J. Millis, A.I. Lichtenstein, A.N. Rubtsov, M. Troyer, P. Werner, Rev. Mod. Phys. **83**, 349 (2011)
39. N.S. Wingreen, Y. Meir, Phys. Rev. B **49**, 11040 (1994). https://doi.org/10.1103/PhysRevB.49.11040
40. E. Lebanon, A. Schiller, Phys. Rev. B **65**, 035308 (2001). https://doi.org/10.1103/PhysRevB.65.035308
41. A. Rosch, J. Paaske, J. Kroha, P. Wölfle, Phys. Rev. Lett. **90**(7), 076804 (2003). https://doi.org/10.1103/PhysRevLett.90.076804
42. J. Paaske, A. Rosch, J. Kroha, P. Wölfle, Phys. Rev. B **70**(15), 155301 (2004). https://doi.org/10.1103/PhysRevB.70.155301
43. A. Rosch, J. Paaske, J. Kroha, P. Wölfle, J. Phys. Soc. Jpn. **74**(1), 118 (2005). https://doi.org/10.1143/JPSJ.74.118. http://jpsj.ipap.jp/link?JPSJ/74/118/
44. J.E. Han, R.J. Heary, Phys. Rev. Lett. **99**, 236808 (2007). https://doi.org/10.1103/PhysRevLett.99.236808
45. F.B. Anders, Phys. Rev. Lett. **101**(6), 066804 (2008). https://doi.org/10.1103/PhysRevLett.101.066804
46. F. Heidrich-Meisner, A.E. Feiguin, E. Dagotto, Phys. Rev. B **79**, 235336 (2009)
47. J. Eckel, F. Heidrich-Meisner, S.G. Jakobs, M. Thorwart, M. Pletyukhov, R. Egger, New. J. Phys. **12**, 043042 (2010)
48. L. Mayrhofer, M. Grifoni, Eur. Phys. J. B **56**(2), 107 (2007). https://doi.org/10.1140/epjb/e2007-00097-3
49. D. Darau, G. Begemann, A. Donarini, M. Grifoni, Phys. Rev. B **79**, 235404 (2009). https://doi.org/10.1103/PhysRevB.79.235404
50. R. Gezzi, T. Pruschke, V. Meden, Phys. Rev. B **75**, 045324 (2007). https://doi.org/10.1103/PhysRevB.75.045324
51. S.G. Jakobs, V. Meden, H. Schoeller, Phys. Rev. Lett. **99**(15), 150603 (2007). https://doi.org/10.1103/PhysRevLett.99.150603
52. H. Schoeller, Eur. Phys. J. Spec. Top. **168**, 179 (2009). https://doi.org/10.1140/epjst/e2009-00962-3
53. P. Werner, T. Oka, M. Eckstein, A.J. Millis, Phys. Rev. B **81**(3), 035108 (2010). https://doi.org/10.1103/PhysRevB.81.035108
54. M.A. Cazalilla, R. Citro, T. Giamarchi, E. Orignac, M. Rigol, Rev. Mod. Phys. **83**, 1405 (2011). https://doi.org/10.1103/RevModPhys.83.1405
55. M. Pletyukhov, H. Schoeller, Phys. Rev. Lett. **108**, 260601 (2012). https://doi.org/10.1103/PhysRevLett.108.260601
56. F. Reininghaus, M. Pletyukhov, H. Schoeller, Phys. Rev. B **90**, 085121 (2014). https://doi.org/10.1103/PhysRevB.90.085121
57. G. Cohen, E. Gull, D.R. Reichman, A.J. Millis, Phys. Rev. Lett. **112**, 146802 (2014). https://doi.org/10.1103/PhysRevLett.112.146802
58. M. Nuss, C. Heil, M. Ganahl, M. Knap, H.G. Evertz, E. Arrigoni, W. von der Linden, Phys. Rev. B **86**, 245119 (2012). https://doi.org/10.1103/PhysRevB.86.245119
59. D. Sexty, T. Gasenzer, J. Pawlowski, Phys. Rev. B **83**, 165315 (2011). https://doi.org/10.1103/PhysRevB.83.165315
60. R. Hützen, S. Weiss, M. Thorwart, R. Egger, Phys. Rev. B **85**, 121408 (2012). https://doi.org/10.1103/PhysRevB.85.121408
61. M. Nuss, M. Ganahl, H.G. Evertz, E. Arrigoni, W. von der Linden, Phys. Rev. B **88**, 045132 (2013). https://doi.org/10.1103/PhysRevB.88.045132

62. M. Knap, E. Arrigoni, W. von der Linden, Phys. Rev. B **88**, 054301 (2013). https://doi.org/10.1103/PhysRevB.88.054301
63. A. Dorda, M. Nuss, W. von der Linden, E. Arrigoni, Phys. Rev. B **89**, 165105 (2014). https://doi.org/10.1103/PhysRevB.89.165105
64. S. Bock, A. Liluashvili, T. Gasenzer, Phys. Rev. B **94**, 045108 (2016). https://doi.org/10.1103/PhysRevB.94.045108
65. A.A. Dzhioev, D.S. Kosov, J. Chem. Phys. **134**, 044121 (2011)
66. T. Prosen, New J. Phys. **10**, 043026 (2008)
67. T. Prosen, J. Stat. Mech. Theory Exp. **2010**(07), P07020 (2010). http://stacks.iop.org/1742-5468/2010/i=07/a=P07020
68. S.A. Gurvitz, Y.S. Prager, Phys. Rev. B **53**, 15932 (1996). https://doi.org/10.1103/PhysRevB.53.15932
69. A.A. Dzhioev, D.S. Kosov, J. Chem. Phys. **135**(17), 174111 (2011). https://doi.org/10.1063/1.3658736. http://link.aip.org/link/?JCP/135/174111/1
70. S. Ajisaka, F. Barra, C. Mejía-Monasterio, T. Prosen, Phys. Rev. B **86**, 125111 (2012). https://doi.org/10.1103/PhysRevB.86.125111
71. A. Dorda, M. Sorantin, W. von der Linden, E. Arrigoni, New J. Phys. **19**(6), 063005 (2017). https://doi.org/10.1088/1367-2630/aa6ccc. http://stacks.iop.org/1367-2630/19/i=6/a=063005
72. H.P. Breuer, Phys. Rev. A **75**, 022103 (2007). https://doi.org/10.1103/PhysRevA.75.022103
73. H.P. Breuer, J. Gemmer, M. Michel, Phys. Rev. E **73**, 016139 (2006). https://doi.org/10.1103/PhysRevE.73.016139
74. W.M. Zhang, P.Y. Lo, H.N. Xiong, M.W.Y. Tu, F. Nori, Phys. Rev. Lett. **109**, 170402 (2012). https://doi.org/10.1103/PhysRevLett.109.170402
75. M.P. Woods, R. Groux, A.W. Chin, S.F. Huelga, M.B. Plenio, J. Math. Phys. **55**(3) (2014). https://doi.org/10.1063/1.4866769
76. I. de Vega, D. Alonso, Rev. Mod. Phys. **89**, 015001 (2017). https://doi.org/10.1103/RevModPhys.89.015001
77. L.M. Sieberer, M. Buchhold, S. Diehl, Rep. Prog. Phys. **79**(9), 096001 (2016). http://stacks.iop.org/0034-4885/79/i=9/a=096001
78. A. Dorda, M. Ganahl, H.G. Evertz, W. von der Linden, E. Arrigoni, Phys. Rev. B **92**, 125145 (2015). https://doi.org/10.1103/PhysRevB.92.125145
79. U. Schollwöck, Ann. Phys. **326**(1), 96 (2011). https://doi.org/10.1016/j.aop.2010.09.012. http://www.sciencedirect.com/science/article/pii/S0003491610001752
80. F. Verstraete, J.J. García-Ripoll, J.I. Cirac, Phys. Rev. Lett. **93**(20), 207204 (2004). https://doi.org/10.1103/PhysRevLett.93.207204. http://link.aps.org/abstract/PRL/v93/e207204
81. M. Zwolak, G. Vidal, Phys. Rev. Lett. **93**(20), 207205 (2004). https://doi.org/10.1103/PhysRevLett.93.207205. http://link.aps.org/abstract/PRL/v93/e207205
82. T. Prosen, M. Znidaric, J. Stat. Mech. **2009**(02), P02035 (2009). http://stacks.iop.org/1742-5468/2009/i=02/a=P02035
83. H.P. Breuer, F. Petruccione, *The Theory of Open Quantum Systems* (Oxford University Press, Oxford, England, 2009). https://global.oup.com/academic/product/the-theory-of-open-quantum-systems-9780199213900
84. G. Schaller, *Open Quantum Systems Far from Equilibrium*. Lecture Notes in Physics (Springer, Heidelberg, 2014). http://www.springer.com/us/book/9783319038766
85. H.J. Carmichael, *Statistical Methods in Quantum Optics: Master Equations and Fokker-Planck Equations, Texts and Monographs in Physics*, vol. 1 (Springer, Singapore, 2002)
86. V. May, O. Kühn, *Charge and Energy Transfer Dynamics in Molecular Systems* (Wiley-VCH, Wennheim, 2011)
87. C.W. Gardiner, P. Zoller, *Quantum Noise* (Springer, Berlin, 2000)
88. C. Cohen-Tannoudji, J. Dupont-Roc, G. Grynberg, Atom-Photon Interactions: Basic Processes and Applications (Wiley-VCH, Weinheim, 2004). https://doi.org/10.1002/9783527617197
89. J. Dalibard, Y. Castin, K. Mølmer, Phys. Rev. Lett. **68**, 580 (1992). https://doi.org/10.1103/PhysRevLett.68.580

90. H.P. Breuer, B. Kappler, F. Petruccione, Phys. Rev. A **56**, 2334 (1997). https://doi.org/10.1103/PhysRevA.56.2334
91. H. Breuer, B. Kappler, F. Petruccione, Eur. Phys. J. B **1**(1), 9 (1998). https://doi.org/10.1007/s100530050058
92. A.J. Daley, J.M. Taylor, S. Diehl, M. Baranov, P. Zoller, Phys. Rev. Lett. **102**, 040402 (2009). https://doi.org/10.1103/PhysRevLett.102.040402
93. Y. Nakamura, Y. Yamanaka, Ann. Phys. **331**, 51 (2013). https://doi.org/10.1016/j.aop.2012.12.005. http://www.sciencedirect.com/science/article/pii/S0003491612002205
94. M. Schmutz, Z. Phys. B **30**, 97 (1978). https://doi.org/10.1007/BF01323673
95. F. Schwarz, M. Goldstein, A. Dorda, E. Arrigoni, A. Weichselbaum, J. von Delft, Phys. Rev. B **94**, 155142 (2016). https://doi.org/10.1103/PhysRevB.94.155142
96. R. van Leeuwen, N.E. Dahlen, G. Stefanucci, C.O. Almbladh, U. von Barth, *Introduction to the Keldysh Formalism* (Springer, Berlin, 2006), *Lecture Notes in Physics*, vol. 706, Chap. 3, pp. 33–59
97. E.N. Economou, *Green's Functions in Quantum Physics* (Springer, Heidelberg, 2006)
98. Y. Meir, N.S. Wingreen, Phys. Rev. Lett. **68**(16), 2512 (1992). http://link.aps.org/abstract/PRL/v68/p2512
99. K. Balzer, S. Hermanns, M. Bonitz, J. Phys. Conf. Ser. **427**(1), 012006 (2013). http://stacks.iop.org/1742-6596/427/i=1/a=012006
100. A.L. Fetter, J.D. Walecka, *Quantum Theory of Many-Particle Systems* (McGraw-Hill, New York, 1971)
101. Y. Saad, *Numerical Methods for Large Eigenvalue Problems, Revised Edition* (Society for Industrial and Applied Mathematics, 2011)
102. P. Arbenz. Lecture notes on solving large scale eigenvalue problems (2012). http://people.inf.ethz.ch/arbenz/ewp/lnotes.html. Online; Accessed May 2016
103. Z. Bai, J. Demmel, J. Dongarra, A. Ruhe, H. van der Vorst, *Templates for the Solution of Algebraic Eigenvalue Problems: A Practical Guide (Software, Environments and Tools)* (Society for Industrial and Applied Mathematics, 1987)